

ADPO: Anchored Direct Preference Optimization

A Unified Framework from Pairwise to Listwise Preferences

Wang Zixian

wangzixian@sd.chinamobile.com

Abstract

Direct Preference Optimization (DPO) has become a standard for aligning models with human feedback, yet its reliance on hard, pairwise preferences makes it brittle to annotator noise and distribution shift. We propose **Anchored Direct Preference Optimization (ADPO)**, a theoretically grounded framework that extends preference learning to soft, listwise supervision through reference anchoring. Our key theoretical contributions are threefold: (1) we establish that ADPO **unifies major learning paradigms**—including supervised fine-tuning, knowledge distillation, maximum-entropy RL, and DPO—as special cases through different choices of target distribution, anchor policy, and temperature; (2) we prove that anchoring induces an implicit trust region governed by the softmax Fisher metric; (3) we formalize the stability of dynamic anchor updates. Empirically, we discover a task-dependent trade-off: dynamic anchors suit online exploration, while fixed anchors excel at offline distillation, reducing teacher-student KL divergence by 2–3 orders of magnitude (170–5000×).

1 Introduction

Preference optimization has become the dominant paradigm for aligning large language models with human values, with Direct Preference Optimization (DPO) [1] emerging as a simple and effective alternative to traditional reinforcement learning from human feedback (RLHF) [2, 3]. However, DPO’s reliance on hard, pairwise preference labels makes it brittle. In noisy settings, this fragility can be severe; our controlled experiments (Section 5) show that under heavy-tailed label noise, DPO’s performance degrades by up to 71% relative to our proposed method (0.472 vs. 0.809 WinMass). This sensitivity arises because DPO’s objective only regularizes the *difference* in log-probabilities, providing a weak inductive bias that is susceptible to overfitting corrupted labels.

To address these limitations, we introduce **Anchored Direct Preference Optimization (ADPO)**, a **unified framework** that reveals a fundamental connection across seemingly disparate learning paradigms. Through a simple anchored projection formulation—minimizing $\text{KL}(q||\tilde{p}_\theta)$ where \tilde{p}_θ is defined via anchored logits $(s - s^{\text{ref}})/\tau$ —we show that supervised fine-tuning, knowledge distillation, maximum-entropy RL policy updates, advantage-weighted methods (AWR/AWAC/MPO), and DPO all emerge as special cases through different choices of target distribution q , anchor policy π_{ref} , and temperature τ (Section 3, Proposition 3.1). The **anchoring structure** is key: by centering the coordinate system at a reference policy before applying softmax, ADPO provides groupwise shift invariance and Fisher-metric regularization—properties absent in standard methods.

We prove that this anchoring mechanism provides a principled geometric framework: the softmax Fisher information metric governs the local curvature around the target distribution (Lemma 3.3), yielding an **implicit trust region** centered at the target (not the anchor itself). This provides a robust, distribution-space analogue to trust-region methods like TRPO [23], without requiring explicit constraints. Crucially, this geometric foundation holds *regardless of anchor choice*, enabling us to investigate the role of the anchor update strategy. To our knowledge, this is the first systematic comparison of a **fixed anchor** (frozen throughout training) versus a **dynamic anchor** (periodically updated to track the current policy) in the context of preference learning and policy optimization. Our central finding is a crucial **task-dependent trade-off**:

- A **dynamic anchor** excels at **online exploration** in noisy environments, where its adaptive trust region improves performance by 5–11% in 3 out of 4 scenarios.
- A **fixed anchor** is dramatically more effective for **offline distillation**, providing a stable target that enables a student model to achieve up to 387% of a teacher’s performance with an astonishing 170–5000× reduction in KL divergence compared to standard knowledge distillation.

Collectively, our work makes four key contributions: (1) we propose ADPO as a **unified projection framework** that subsumes major learning paradigms (SFT, KD, max-ent RL, DPO) and robustly handles soft and listwise data; (2) we establish the theoretical connection between anchoring and implicit, Fisher-metric trust regions; (3) we uncover the task-dependent trade-off between anchor strategies, a key practical insight; and (4) we provide extensive empirical evidence and clear guidance for selecting anchor strategies in different learning contexts, informing both online RLHF and offline distillation pipelines.

2 Related Work

Preference optimization. More generally, the Preference Optimization (PO) framework [18] formulates an entropy-regularized objective aligning policy probabilities with qualitative preference signals, which inspires our entropy-regularized interpretation of anchoring (Section 3), though our work focuses on preference optimization for RLHF-style alignment rather than combinatorial optimization. DPO [1] reparameterizes the reward model through policy-reference log-ratios, enabling direct optimization. Extensions include identity-free preferences (IPO [5]), contrastive objectives (CPO [6]), and iterative refinement [7]. Our work provides a unified framework encompassing these variants.

Listwise preference learning. Plackett–Luce models [9, 10] enable listwise preferences through recursive top-1 selections. Recent work applies PL to LLM alignment [11, 12, 13]. We extend DPO to listwise settings through reference anchoring.

Robust learning under noise. Prior work addresses noise through majority voting [15], uncertainty quantification [16], and robust reward learning [17]. Our approach encodes uncertainty in soft probabilities and provides anchoring for groupwise shift invariance.

Relation to KD and TRPO. Conventional knowledge distillation (KD) [22] aligns a student with a teacher by minimizing $\text{KL}(q||p_\theta)$, which directly matches absolute probabilities in the Euclidean probability space. While effective, this objective lacks a fixed geometric center and thus provides no notion of a trust region, making it sensitive to teacher noise and distributional shifts. In contrast, trust-region policy optimization (TRPO) [23] explicitly constrains $\text{KL}(\pi_{\theta_{\text{old}}}||\pi_\theta)$ in the *parameter space*, defining a moving local quadratic region that stabilizes updates. Our ADPO formulation can be viewed as a *distribution-space analogue* of TRPO: by anchoring logits to a reference policy, the optimization is performed in a coordinate system whose origin is fixed at the reference. This anchoring keeps the Fisher metric centered and effectively forms a “quadratic bowl” around the reference distribution, yielding an implicit trust region without any explicit KL constraint. To our knowledge, no prior work has formulated such an anchored cross-entropy that maintains a fixed geometric center in probability space.

Entropy-regularized grounding and its link to ADPO. Under the maximum-entropy RL objective

$$\max_{\pi} \mathbb{E}_{x \sim \mathcal{D}} \left[\mathbb{E}_{\tau \sim \pi(\cdot|x)} r(x, \tau) + \alpha \text{H}(\pi(\cdot|x)) \right],$$

the optimal policy admits the Boltzmann form [19, 21]

$$\pi^*(\tau|x) = \frac{1}{Z(x)} \exp\left(\frac{1}{\alpha} r(x, \tau)\right), \quad (1)$$

and the reward can be reparameterized by the (optimal) policy log-probability

$$r(x, \tau) = \alpha \log \pi^*(\tau|x) + \alpha \log Z(x), \quad (2)$$

so any *relative* quantity (pairwise/listwise) cancels $Z(x)$. Eqs. (1)–(2) yield a direct bridge between reward differences and policy log-odds: Bradley–Terry and Plackett–Luce targets arise by mapping Δr to a preference probability via a sigmoid/softmax, while ADPO matches the student’s *anchored* log-odds $(s - s^{\text{ref}})/\tau$ to these soft targets. A full derivation of (1) as the minimizer of $\mathbb{E}_x \text{KL}(\pi(\cdot|x) \parallel \pi^*(\cdot|x))$ and the log-partition cancellation in pairwise/listwise forms can be found in [18] (see their Eqs. (3)–(6), (20)–(27)).

Lemma 2.1 (Groupwise shift invariance). *If $r'(x, \tau) = r(x, \tau) - h(x)$ for any function h independent of τ , then π^* in (1) is unchanged; hence all pairwise/listwise probabilities (BT/PL) are identical, and anchored ADPO—which operates on $(s - s^{\text{ref}})$ —inherits groupwise shift invariance. See [18], Prop. 3.1 and App. D.2.*

3 Anchored Direct Preference Optimization

Notation. Throughout this section, we use the following notation:

- x : context (prompt/state); $S_x = \{1, \dots, |S_x|\}$: candidate set (actions/outputs)
- $\pi_\theta(i | x)$: student policy probability for candidate i given context x
- $\pi_{\text{ref}}(i | x)$: reference (anchor) policy, either fixed or dynamic
- $s_i = \log \pi_\theta(i | x)$, $s_i^{\text{ref}} = \log \pi_{\text{ref}}(i | x)$: log-probabilities
- $q(i | S_x)$: target preference distribution over candidates (from teacher, rewards, or labels)
- $u_i = (s_i - s_i^{\text{ref}})/\tau$: anchored logits
- $\tilde{p}_\theta(i | S_x) = \text{softmax}(u)$: anchored model distribution

Table 1: **Temperature parameters and their roles across ADPO formulations.**

Symbol	Role	Where used
β_r	Teacher/target inverse temperature	Forms q from rewards: $q \propto \exp(R/\beta_r)$
β	Student inverse temperature (pairwise)	Pairwise logistic: $\sigma(\beta(\Delta_\theta - \Delta_{\text{ref}}))$
τ	Anchoring temperature	Defines anchored logits: $u = (s - s^{\text{ref}})/\tau$ (listwise)

Remark (scale non-identifiability): In pairwise settings, temperatures β and β_r only appear through their ratio β_r/β in the Bayes-optimal condition, so the *statistical optimum* is invariant to jointly rescaling them. We set $\beta = \beta_r = 1.0$ by default. However, the *optimization dynamics* are affected: *pairwise* gradients scale as β (since $\partial \ell / \partial \theta = \beta(\sigma(\beta(\Delta_\theta - \Delta_{\text{ref}})) - q_{ij})(\nabla s_i - \nabla s_j)$), while *listwise* gradients scale as $1/\tau$ (because $\partial \mathcal{L} / \partial s_i = \frac{1}{\tau}(\tilde{p} - q)$). Thus smaller β slows pairwise updates; smaller τ tightens the trust region via curvature $\propto 1/\tau^2$ but increases gradient magnitudes.

Remark (temperature τ and regularization strength): In listwise settings with anchoring, τ controls the balance between the anchor and target via the closed-form solution $\pi_\theta \propto \pi_{\text{ref}} \cdot q^\tau$ (Proposition 3.2). Intuitively:

- As $\tau \rightarrow 0$: $q^\tau \rightarrow \mathbf{1}$ (uniform), so $\pi_\theta \rightarrow \pi_{\text{ref}}$ (stronger regularization toward the anchor).
- As $\tau \rightarrow \infty$: q^τ becomes increasingly peaked at $\arg \max q$, so π_θ tracks the target q more aggressively.

Note that \tilde{p}_θ always matches q at optimality regardless of τ ; the temperature affects how the underlying policy π_θ relates to the anchor. Smaller τ induces a tighter implicit trust region in the sense that large deviations $\log(\pi_\theta/\pi_{\text{ref}})$ are more heavily penalized (since gradients scale as $1/\tau$).

3.1 ADPO as a Unified Anchored Projection

We cast preference learning as an *anchored projection* on the probability manifold: given target q and anchor π_{ref} , minimizing $\text{KL}(q \parallel \tilde{p}_\theta)$ aligns the student under the softmax Fisher geometry. This unified view encompasses supervised fine-tuning, knowledge distillation, maximum-entropy RL, and DPO as special cases.

Master formulation. Given student π_θ , anchor π_{ref} , and temperature $\tau > 0$, the *anchored logits* are

$$u_i = \frac{s_i - s_i^{\text{ref}}}{\tau}, \quad s_i = \log \pi_\theta(i | x), \quad s_i^{\text{ref}} = \log \pi_{\text{ref}}(i | x). \quad (3)$$

Note (sequence models): In autoregressive sequence models, we use length-normalized log-probabilities (token-average NLL) for s and s^{ref} to avoid length bias. Under this setting, each candidate’s score is the per-token average, and these averaged scores enter the group-level softmax over candidates. Since length normalization amounts to an equal rescaling of all scores within a group, it preserves the softmax affine-invariance: the Fisher geometry and anchoring properties remain intact when applied to this *sequence-level* distribution over candidates (not the token-level distribution). Thus the theoretical results—groupwise shift invariance (Lemma 2.1), implicit trust region (Lemma 3.3), and closed-form projection (Proposition 3.2)—carry through in this setting. The anchored model distribution over a group S_x is

$$\tilde{p}_\theta(i | S_x) = \frac{\exp(u_i)}{\sum_{j \in S_x} \exp(u_j)} = \text{softmax}_i \left(\frac{\log \pi_\theta(i | x) - \log \pi_{\text{ref}}(i | x)}{\tau} \right). \quad (4)$$

Given a target preference distribution $q(\cdot | S_x)$ (pairwise or listwise), **ADPO** minimizes

$$\mathcal{L}_{\text{ADPO}} = \mathbb{E}_{x, S_x} [\text{KL}(q(\cdot | S_x) \parallel \tilde{p}_\theta(\cdot | S_x))] = \mathbb{E}_{x, S_x} \left[- \sum_{i \in S_x} q(i | S_x) \log \tilde{p}_\theta(i | S_x) \right] + \text{const.} \quad (5)$$

This objective performs a projection onto the anchored probability manifold; its second-order expansion around q yields the softmax Fisher metric, inducing an *implicit trust region* centered at π_{ref} (formalized in Section 3.4).

Relation to standard DPO. DPO [1] also introduces a reference model, but it enters only through *log-odds differences* between two candidates:

$$\Delta_{\theta, \text{ref}} = (\log \pi_\theta - \log \pi_{\text{ref}})_{y_i} - (\log \pi_\theta - \log \pi_{\text{ref}})_{y_j}.$$

In contrast, ADPO anchors *each* score $s_i - s_i^{\text{ref}}$ individually before normalizing across the group to form \tilde{p}_θ . When $|S_x| = 2$ and q is binary (or Bradley–Terry soft targets), Eq. (5) reduces to the logistic preference loss used in DPO. For general listwise $|S_x| > 2$, ADPO retains distribution-level anchoring and inherits a Fisher-metric trust region around π_{ref} .

Proposition 3.1 (ADPO unifies major learning paradigms). *Let $\mathcal{L}_{\text{ADPO}}$ be defined in Eq. (5). Different choices of target q , anchor π_{ref} , and temperature τ recover:*

1. **Supervised fine-tuning (SFT).** *If $q(\cdot | S_x)$ equals the data label distribution (one-hot or soft), π_{ref} is uniform (constant logits that cancel in softmax), and $\tau = 1$, then $\tilde{p}_\theta = \pi_\theta$ and $\mathcal{L}_{\text{ADPO}} = \mathbb{E}[\text{CE}(q, \pi_\theta)]$, the standard cross-entropy loss. For $\tau \neq 1$, \tilde{p}_θ is a temperature-scaled version of π_θ .*
2. **Knowledge distillation (KD).** *If $q = \text{softmax}(z_T/T)$ is the teacher softened by temperature T , π_{ref} is uniform, and we set $\tau = T$ with loss $T^2 \cdot \mathcal{L}_{\text{ADPO}}$ (where T^2 preserves gradient magnitude), this recovers standard KD [22]. Training uses $T > 1$; inference restores $T = 1$. If instead $\pi_{\text{ref}} = \pi_T$, we obtain anchored KD where the optimization is performed in teacher-anchored coordinates—our distillation experiments (Section 5.5) show this achieves 170–5000× lower KL divergence.*

3. Maximum-entropy RL / offline policy projection.

- **(Soft-optimal Boltzmann policy)** The standard maximum-entropy RL objective yields the soft-optimal policy $\pi^*(a|s) \propto \exp(Q(s, a)/\alpha)$ [19, 21, 20]. To match this target via ADPO’s anchored distribution \tilde{p}_θ , we set $q(a|s) \propto \exp(Q(s, a)/\alpha)$ and use a uniform anchor π_{ref} .

Parametrization: ADPO constrains the anchored distribution $\tilde{p}(u) = \text{softmax}((\log \pi_\theta - \log \pi_{\text{ref}})/\tau)$ to equal q . Since there are equivalent parameterizations, we choose $\tau = 1$ and $\pi_\theta(a|s) \propto \pi_{\text{ref}}(a|s) \exp(Q(s, a)/\alpha)$ (with π_{ref} uniform, this reduces to $\pi_\theta \propto \exp(Q/\alpha)$). This directly recovers the standard soft-optimal policy π^* for use in sampling/evaluation, preserving the conventional Boltzmann temperature $1/\alpha$. Alternative parameterizations (e.g., $\tau = \alpha$ with $\pi_\theta \propto \exp(Q)$) yield the same \tilde{p} but would shift the temperature into the anchoring scale, which we avoid for clarity.

- **(AWR/AWAC/MPO advantage-weighted projection)** When S_x is the full action space with overlapping support between π_{old} and the target q , the anchor is $\pi_{\text{ref}} = \pi_{\text{old}}$, and the target is $q(a|s) \propto \pi_{\text{old}}(a|s) \exp(A^{\pi_{\text{old}}}(s, a)/\beta)$ where $A^{\pi_{\text{old}}} = Q^{\pi_{\text{old}}} - V^{\pi_{\text{old}}}$ (shift-invariant to constant baselines), with $\tau = \beta$. The optimal anchored distribution is $\tilde{p}_\theta = q \propto \pi_{\text{old}} \exp(A/\beta)$, exactly matching the advantage-weighted target.

Derivation of π_θ form: ADPO enforces $\tilde{p}(u) = q$ with $u = (\log \pi_\theta - \log \pi_{\text{old}})/\tau$ and $\tau = \beta$. Then

$$\tilde{p}(u) \propto \exp\left(\frac{\log \pi_\theta - \log \pi_{\text{old}}}{\beta}\right) \stackrel{!}{\propto} \pi_{\text{old}} \exp(A/\beta),$$

which is equivalent to

$$\frac{\pi_\theta}{\pi_{\text{old}}} \propto \left(\pi_{\text{old}} e^{A/\beta}\right)^\beta \Rightarrow \pi_\theta \propto \pi_{\text{old}}^{1+\beta} e^A.$$

What is exactly recovered? ADPO matches the **anchored** distribution \tilde{p} to the advantage-weighted target q ; the induced policy shape $\pi_\theta \propto \pi_{\text{old}}^{1+\beta} \exp(A)$ is a consequence of the anchored projection (Prop. 3.2) and is not the classic MPO/AWAC M-step update (which yields $\pi_\theta \propto \pi_{\text{old}} \exp(A/\beta)$ or directly $\pi_\theta = q$ under sufficient capacity). Our equivalence is thus at the \tilde{p} -level rather than the π_θ -level. **Assumptions:** (1) full action space S_x is enumerable or covered by samples; (2) advantage weights $\exp(A/\beta)$ are normalizable; (3) for off-policy data d^β , we approximate by ignoring or clipping importance ratios (standard in AWR/AWAC [24, 25]), yielding weighted MLE $\max_\theta \mathbb{E}_{(s,a) \sim d^\beta} [\exp(A/\beta) \log \pi_\theta(a|s)]$. MPO’s E-step weights $w \propto \exp(Q/\eta)$ with dual variable η (enforcing a KL constraint via Lagrangian duality) follow the same projection form [26], though MPO additionally solves for η to satisfy a KL budget.

4. **DPO (binary comparison form).** For $|S_x| = 2$ with candidates $\{i, j\}$ and Bradley–Terry soft targets $q(i | \{i, j\}) = \sigma(\beta_r \Delta R)$ where $\Delta R = R_i - R_j$ is the reward difference, Eq. (5) is equivalent to DPO up to temperature scaling and reference shift. Specifically, the Bayes-optimal condition $\sigma(\beta(\Delta_\theta - \Delta_{\text{ref}})) = q_{ij}$ yields $\Delta_\theta - \Delta_{\text{ref}} = (\beta_r/\beta)\Delta R$. When $\beta = \beta_r$ and π_{ref} is uniform (so $\Delta_{\text{ref}} = 0$), this is exactly identical to the original DPO objective; otherwise, it differs by a temperature rescaling β_r/β and an anchor-induced shift Δ_{ref} .

Proposition 3.2 (Closed-form optimal solution). Suppose S_x covers the full action/class space and $q(\cdot | S_x) \succ 0$. **(Discrete case)** If the policy π_θ has sufficient expressivity (i.e., the parametrization can represent arbitrary log-odds over S_x), then the distribution-level optimum of $\arg \min_\theta \text{KL}(q || \tilde{p}_\theta)$ satisfies

$$\pi_\theta(i | x) \propto \pi_{\text{ref}}(i | x) \cdot q(i | x)^\tau. \quad (6)$$

(Continuous case) For continuous action spaces, assume q , π_θ , and π_{ref} admit densities with respect to a common base measure (e.g., Lebesgue measure). Define the anchored distribution via the density ratio:

$$\tilde{p}_\theta(a) \propto \exp\left(\frac{\log \pi_\theta(a) - \log \pi_{\text{ref}}(a)}{\tau}\right) = \left(\frac{\pi_\theta(a)}{\pi_{\text{ref}}(a)}\right)^{1/\tau}.$$

Table 2: **ADPO as a unifying projection framework.** Different choices of target q , anchor π_{ref} , and temperature τ recover major learning paradigms. **Key:** Optimization matches the *anchored distribution* $\tilde{p}_\theta = \text{softmax}((s - s^{\text{ref}})/\tau)$ to the target q ; the corresponding *student policy* π_θ satisfies $\pi_\theta \propto \pi_{\text{ref}} \cdot q^\tau$ when the optimum is reachable (Prop. 3.2).

Task	Target $q(\cdot x)$	Anchor π_{ref}	τ	Recovers ($\tilde{p}_\theta / \pi_\theta$)
SFT	data (one-hot/soft)	uniform	1	cross-entropy / same
KD (standard)	$\text{softmax}(z_T/T)$	uniform	T	$T^2 \text{CE}(q_T, \text{softmax}(s/T))$ / train at T , infer $T=1$
KD (anchored)	teacher π_T	π_T	any	$\text{KL}(\pi_T \ \text{softmax}((s - s_T)/\tau))$ / trust region
Max-ent RL	$\propto \exp(Q/\alpha)$	uniform	1	$q / \propto \exp(Q/\alpha)$
Adv.-wtd RL	$\propto \pi_{\text{old}} \exp(A/\beta)$	π_{old}	β	$q / \propto \pi_{\text{old}}^{1+\beta} \exp(A)$ (matches q in \tilde{p} -space)
DPO (binary)	Bradley–Terry / hard	uniform	any	original DPO (pairwise)
ADPO (listwise)	Plackett–Luce / soft	any (teacher/old)	any	this work

Setting $\tilde{p}_\theta = q$ yields the closed-form solution

$$\pi_\theta(a) \propto \pi_{\text{ref}}(a) \cdot q(a)^\tau,$$

which requires: (i) overlapping support: $q(a) > 0 \Rightarrow \pi_{\text{ref}}(a) > 0$ almost everywhere; (ii) integrability: $\int \pi_{\text{ref}}(a) \cdot q(a)^\tau da < \infty$ to ensure normalizability. Under these conditions, the solution is unique up to the normalization constant (equivalently, the Radon–Nikodym derivative $d\pi_\theta/d\mu$ is determined by the multiplicative form, where μ is the base measure).

Proof (discrete): $\tilde{p}_\theta = \text{softmax}((s - s^{\text{ref}})/\tau) = q$ if and only if $(s - s^{\text{ref}})/\tau = \log q + c\mathbf{1}$ for some constant c (reflecting the shift-invariance of softmax), which rearranges to $\pi_\theta \propto \pi_{\text{ref}} q^\tau$. The constant c is absorbed into the proportionality constant. \square

Implication and reachability. Equation (6) strictly characterizes the "anchored projection" as a *multiplicative fusion* of reference and target when the optimum is reachable. In discrete finite-action settings with tabular or sufficiently expressive function approximation, this optimum is exactly attainable. However, in structured settings (e.g., autoregressive language models with shared parameters across tokens, or policy networks with limited capacity), the optimum may be unreachable, and gradient descent performs an approximate projection in the parametric family. The KD, MaxEnt, and AWR special cases in Proposition 3.1 all follow directly from (6).

Listwise subset constraints and convexity. When S_x is only a subset (pairwise/listwise ranking), (6) holds *within each group*, but the global π_θ must simultaneously satisfy multiple group constraints. Crucially, $\mathcal{L}_{\text{ADPO}}$ is convex with respect to the anchored logits $u = (s - s^{\text{ref}})/\tau$ within each group (as shown in Theorem 3.6), but the optimization over shared parameters θ is typically *non-convex*. The group-wise closed-form solution provides a target, but there may not exist a parameter θ that simultaneously achieves $\tilde{p}_\theta(\cdot | S_x) = q(\cdot | S_x)$ for all groups (except in the tabular case or with unlimited expressivity). Thus, in practice, ADPO performs a parameterized fitting that minimizes the expected group-wise KL, balancing the constraints across all training groups.

By centering the coordinate system at π_{ref} before applying softmax, ADPO provides groupwise shift invariance (Lemma 2.1) and Fisher-metric regularization (Lemma 3.3)—properties absent in standard KD or unanchored DPO. Table 2 summarizes the unification.

Standing assumptions. Throughout this work, we maintain the following conditions unless otherwise noted:

- (i) **Support overlap (discrete):** For discrete action/candidate spaces, we assume $q(i|x) > 0 \Rightarrow \pi_{\text{ref}}(i|x) > 0$ for all $i \in S_x$, ensuring that anchored logits $u_i = (s_i - s_i^{\text{ref}})/\tau$ are well-defined.
- (ii) **Absolute continuity (continuous):** For continuous action spaces, we assume q , π_θ , and π_{ref} admit densities with respect to a common base measure, with overlapping support in the same sense as (i).

- (iii) **Local analysis vs. global bounds:** Fisher-metric trust region results (Lemma 3.3, Corollary 3.4) hold *locally* around u^* where $\tilde{p}_\theta(u^*) = q$. For global strong convexity, we either work in a neighborhood of u^* or assume the optimization is constrained to a bounded domain where $\tilde{p}_\theta(u)_i \in [\varepsilon, 1 - \varepsilon]$ (Theorem 3.6).
- (iv) **Sequence models:** For autoregressive sequence generation, we use length-normalized (per-token average) log-probabilities s and s^{ref} as group-level scores, and apply the softmax Fisher geometry at the *sequence-level* distribution over candidates.
- (v) **Expressivity:** Closed-form optimal solutions (Proposition 3.2) assume the policy parametrization π_θ has sufficient expressivity to represent the target multiplicative form $\pi_{\text{ref}} \cdot q^\tau$. In practice (e.g., shared-parameter networks, autoregressive models), we perform an approximate projection in the parametric family.

3.2 Pairwise Instantiation

Notation for this subsection: β = student inverse temperature, β_r = teacher/reference inverse temperature, q_{ij} = soft preference probability that $i \succ j$.

For a candidate pair (i, j) with soft teacher preference $q_{ij} \in (0, 1)$ that i is preferred, the ADPO pairwise loss is:

$$\ell_{ij}^{\text{Soft-DPO}} = \log \left(1 + e^{\beta(\Delta_\theta - \Delta_{\text{ref}})} \right) - q_{ij} \beta(\Delta_\theta - \Delta_{\text{ref}}), \quad (7)$$

where $\beta > 0$ is student temperature, $\Delta_\theta = s_i - s_j$, and $\Delta_{\text{ref}} = s_i^{\text{ref}} - s_j^{\text{ref}}$ with $s_i = \log \pi_\theta(\tau_i | x)$.

Key properties:

- **Bayes-optimal matching:** Gradient vanishes when $\sigma(\beta(\Delta_\theta - \Delta_{\text{ref}})) = q_{ij}$.
- **Soft weighting:** Uncertain pairs ($q_{ij} \approx 0.5$) contribute less gradient.
- **Reference anchoring:** Relative updates $\Delta_\theta - \Delta_{\text{ref}}$ are invariant to groupwise shifts.

3.3 Listwise Instantiation

Notation for this subsection: τ = anchor temperature, β_r = teacher inverse temperature for forming q from rewards, \tilde{R}_i = observed rewards, \hat{R}_i = transformed rewards.

For group $S_x = \{\tau_1, \dots, \tau_P\}$, the ADPO listwise loss is:

$$\mathcal{L}_{\text{group}}^{\text{ref}} = \mathbb{E}_{x, S_x} \left[- \sum_{i \in S_x} q(i | S_x) \log \tilde{p}_\theta(i | S_x) \right], \quad (8)$$

where

$$\tilde{p}_\theta(i | S_x) = \frac{\exp((s_i - s_i^{\text{ref}})/\tau)}{\sum_{j \in S_x} \exp((s_j - s_j^{\text{ref}})/\tau)}, \quad (9)$$

and teacher target $q(i | S_x) \propto \exp(\hat{R}_i / \beta_r)$ uses transformed rewards \hat{R}_i via: (a) raw: $\hat{R}_i = \tilde{R}_i$; (b) rank-based Gaussian transform; or (c) KDE-CDF-Logit: $\hat{R}_i = \text{logit}(\hat{F}(\tilde{R}_i))$ where \hat{F} is the KDE-estimated CDF.

Equivalent expansion. The anchored listwise cross-entropy (8) can be equivalently written as:

$$- \sum_{i \in S_x} q(i | S_x) \log \tilde{p}_\theta(i | S_x) = -\frac{1}{\tau} \sum_{i \in S_x} q(i | S_x) (s_i - s_i^{\text{ref}}) + \log \sum_{j \in S_x} \exp\left(\frac{s_j - s_j^{\text{ref}}}{\tau}\right). \quad (10)$$

This decomposition makes explicit that the anchored listwise cross-entropy consists of a linear matching term $-\langle q, (s - s^{\text{ref}})/\tau \rangle$ and a log-sum-exp normalization. It directly reveals the connection to the convex conjugate form of the softmax, underlying the implicit trust-region regularization discussed below. Since $\text{KL}(q \| \tilde{p}_\theta) = \mathcal{L}_{\text{group}}^{\text{ref}} + H(q)$ and $H(q)$ is parameter-independent, minimizing (10) is equivalent to minimizing the KL divergence from the teacher distribution q to the student's anchored distribution \tilde{p}_θ .

3.4 Fisher Geometry and Implicit Trust Region

We now formalize how anchoring provides an implicit trust region through Riemannian geometry.

Lemma 3.3 (Implicit trust region; quadratic form at $p = q$). *Let $u = (s - s^{\text{ref}})/\tau$ and $\tilde{p}(u) = \text{softmax}(u)$. Let $u^\star = \log q + c\mathbf{1}$ so that $\tilde{p}(u^\star) = q$ (the softmax is shift-invariant). Define $\delta = u - u^\star$ and center it by q as $\bar{\delta} = \delta - \langle q, \delta \rangle \mathbf{1}$. Then, as $u \rightarrow u^\star$,*

$$\text{KL}(q \parallel \tilde{p}(u)) = \frac{1}{2} \bar{\delta}^\top (\text{Diag}(q) - qq^\top) \bar{\delta} + o(\|\bar{\delta}\|^2) = \frac{1}{2\tau^2} \text{Var}_{i \sim q}[(s_i - s_i^{\text{ref}}) - \tau \log q_i] + o(\cdot),$$

where the variance is taken with respect to q , measuring the deviation of the anchored log-odds from the target q . The quadratic form uses the softmax Fisher metric $\text{Diag}(q) - qq^\top$, which has a null-space along $\mathbf{1}$ (reflecting shift-invariance).

Proof sketch. Let $A(u) = \log \sum_j e^{u_j}$ so that $\mathcal{L}(u) = A(u) - \langle q, u \rangle$. Then $\nabla A(u) = \tilde{p}_\theta(\cdot; u)$ and $\nabla^2 A(u) = \text{Diag}(\tilde{p}_\theta) - \tilde{p}_\theta \tilde{p}_\theta^\top$. A second-order Taylor expansion of \mathcal{L} at u^\star with $\tilde{p}_\theta(\cdot; u^\star) = q$ yields the stated quadratic form. The centering removes the null-space along $\mathbf{1}$, reflecting the invariance of softmax to additive shifts. \square

Corollary 3.4 (Local bounds). *Let $\mu(q) > 0$ denote the smallest nonzero eigenvalue of $\text{Diag}(q) - qq^\top$ (the null-space is along $\mathbf{1}$). Then locally around u^\star ,*

$$\text{KL}(q \parallel \tilde{p}(u)) \geq \frac{\mu(q)}{2} \|\bar{\delta}\|^2,$$

where $\bar{\delta} = \delta - \langle q, \delta \rangle \mathbf{1}$ is the q -centered deviation. By Pinsker's inequality, $\|\tilde{p}(u) - q\|_1 \leq \sqrt{2\text{KL}(q \parallel \tilde{p}(u))}$, providing a distributional deviation bound.

On the smallest nonzero eigenvalue: For $K = 2$, $\mu(q) = 2q(1 - q)$. For $K > 2$, $\mu(q)$ depends on the full spectrum of q ; a uniform, distribution-independent lower bound is generally loose. When $\min_i q_i \geq \varepsilon > 0$, the smallest nonzero eigenvalue satisfies $\mu(q) \geq \varepsilon$. Proof sketch: For any $v \in \mathbf{1}^\perp$, the Rayleigh quotient gives $v^\top (\text{Diag}(q) - qq^\top) v = \sum_i q_i v_i^2 - (\sum_i q_i v_i)^2 = \text{Var}_q[v] \geq \varepsilon \|v\|^2$ since $\sum_i v_i = 0$ and the variance of v under any distribution bounded below by ε is at least $\varepsilon \|v\|^2$.

Geometric interpretation. ADPO performs optimization in the anchored u -coordinate system: the reference π_{ref} defines the coordinate origin via $u = (s - s^{\text{ref}})/\tau$, but the center of the local quadratic bowl is at u^\star satisfying $\tilde{p}_\theta(\cdot; u^\star) = q(\cdot)$, not at the anchor itself. The local curvature at u^\star is governed by the softmax Fisher metric $\text{Diag}(q) - qq^\top$, which depends only on the target q . Thus: the anchor determines the coordinate system, while the target q determines both the minimizer u^\star and the local geometry. This contrasts with:

- **Knowledge Distillation (KD):** Minimizes $\text{KL}(q \parallel p_\theta)$ in the Euclidean probability simplex. While the Fisher curvature exists at any point, there is no fixed reference anchor, so the geometry lacks a stable coordinate origin.
- **TRPO:** Constrains $\text{KL}(\pi_{\theta_{\text{old}}} \parallel \pi_\theta)$ in parameter space, defining a moving local quadratic region that requires explicit constraint optimization.
- **ADPO:** Anchoring logits to s^{ref} yields a distribution-space analogue of TRPO with a fixed coordinate origin, inducing an implicit trust region without explicit constraints.

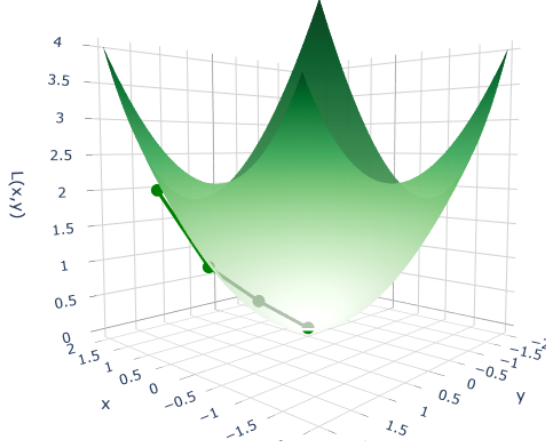


Figure 1: **ADPO’s anchored trust region.** The Fisher metric $\text{Diag}(q) - qq^\top$ induces a quadratic “bowl” in the distribution space, expressed in anchored coordinates $u = (s - s^{\text{ref}})/\tau$; the quadratic well is centered at u^* (i.e., at the target q), not at the anchor itself. The green trajectory shows the optimization path descending toward the optimal policy, with the anchored coordinate system providing an implicit trust region that prevents large distributional drift. This geometric structure holds for both fixed anchors (stable centers for distillation) and dynamic anchors (adaptive regions for exploration).

3.5 Geometric Interpretation: KL-Mirror Descent in u -Space

Recall $A(u) = \log \sum_j \exp(u_j)$ and $\tilde{p}(u) = \nabla A(u) = \text{softmax}(u)$, and our anchored objective $\mathcal{L}(u) = A(u) - \langle q, u \rangle = \text{KL}(q \parallel \tilde{p}(u)) + H(q)$. Let u_t be the current anchored logits and $g_t = \nabla \mathcal{L}(u_t) = \tilde{p}(u_t) - q$.

Theorem 3.5 (KL-mirror descent / Bregman-prox step in u -space). *If one were to directly optimize \mathcal{L} over the anchored logits u (rather than shared parameters θ), then for any step size $\eta > 0$, the one-step update can be written equivalently as the solution of the following proximal subproblem:*

$$u_{t+1} = \arg \min_u \langle g_t, u \rangle + \frac{1}{\eta} \text{KL}(\tilde{p}(u_t) \parallel \tilde{p}(u)). \quad (11)$$

Equivalently, since $D_A(u \parallel u_t) = A(u) - A(u_t) - \langle \nabla A(u_t), u - u_t \rangle = \text{KL}(\tilde{p}(u_t) \parallel \tilde{p}(u))$, (11) is a standard mirror descent / Bregman-prox step with generator A .

Proof. Linearize \mathcal{L} at u_t : $\mathcal{L}(u) \approx \mathcal{L}(u_t) + \langle g_t, u - u_t \rangle$. A mirror descent step with generator A minimizes $\langle g_t, u \rangle + \frac{1}{\eta} D_A(u \parallel u_t)$. Using $D_A(u \parallel u_t) = \text{KL}(\tilde{p}(u_t) \parallel \tilde{p}(u))$ for the softmax family yields (11). \square \square

Dual form in p -space. Via the Legendre map $p = \nabla A(u)$, the step (11) is equivalent to the entropic proximal in probability space

$$\tilde{p}_{t+1} = \arg \min_{p \in \Delta} \langle g_t, p \rangle + \frac{1}{\eta} \text{KL}(p \parallel \tilde{p}_t),$$

whose solution is the multiplicative-weights update $\tilde{p}_{t+1} \propto \tilde{p}_t \odot \exp(-\eta g_t)$.

Multiplicative-weights view. The solution of (11) is equivalent to the multiplicative-weights update in the anchored distribution:

$$\tilde{p}_{t+1} \propto \tilde{p}_t \odot \exp(-\eta g_t) = \tilde{p}_t \odot \exp(-\eta(\tilde{p}_t - q)), \quad (12)$$

followed by renormalization. This exhibits ADPO as a KL-trust-region step in distribution space.

Step-size η vs temperature τ (heuristic). Anchored coordinates $u = (s - s^{\text{ref}})/\tau$ rescale curvature by $1/\tau^2$ (Lemma 3.3). To maintain comparable “trust-region tightness” in the *unanchored* score space s , one may heuristically choose

$$\eta \propto \tau^2 \quad (\text{decreasing } \tau \text{ calls for a quadratic decrease of } \eta). \quad (13)$$

This is a practical guideline; a rigorous derivation would require accounting for the chain rule $\partial u/\partial \theta$ when optimizing over shared parameters θ .

3.6 Dynamic Anchor Stability

Crucially, Lemma 3.3 holds *regardless of anchor choice*. The Fisher metric $\text{Diag}(q) - qq^\top$ automatically constrains optimization to a local quadratic region. While the coordinate $u = (s - s^{\text{ref}})/\tau$ depends on the anchor, the local quadratic form at the optimum only depends on q ; thus the curvature (Fisher metric) is anchor-agnostic, albeit the optimization objective itself changes with the anchor. Common anchor choices include:

- **Fixed anchor:** A reference π_{ref} pre-trained and frozen throughout training, providing a *stable coordinate origin* for consistent target tracking;
- **Dynamic anchor:** A policy $\pi_{\theta_{\text{old}}}$ that periodically updates to the current policy (every K epochs via $\pi_{\text{ref}} \leftarrow \pi_\theta$), providing an *adaptive coordinate system* similar to TRPO’s old-policy mechanism;
- **Teacher anchor:** A stronger teacher π_{teacher} for offline distillation (typically fixed).

For dynamic anchors, we characterize the monotonic improvement *within each fixed-anchor phase*:

Theorem 3.6 (Fixed-anchor-phase monotonic descent in u -space). *Consider a training phase where the anchor π_{ref} is held fixed. Define $\mathcal{L}(u) = A(u) - \langle q, u \rangle$ where $A(u) = \log \sum_j e^{u_j}$ and $u = (s - s^{\text{ref}})/\tau$ are the anchored logits. When directly optimizing \mathcal{L} over u (e.g., tabular setting or each group having independent degrees of freedom), \mathcal{L} is strictly convex on the subspace $\mathbf{1}^\perp$ (orthogonal to the all-ones vector) with Hessian $\nabla^2 \mathcal{L}(u) = \text{Diag}(\tilde{p}_\theta(u)) - \tilde{p}_\theta(u)\tilde{p}_\theta(u)^\top$, which is positive semidefinite on $\mathbf{1}^\perp$ with one zero eigenvalue along $\mathbf{1}$.*

Strong convexity (local or bounded-domain):

- **Local:** *In a neighborhood of u^\star (where $\tilde{p}_\theta(u^\star) = q$), the Hessian $\nabla^2 \mathcal{L}(u) = \text{Diag}(\tilde{p}_\theta(u)) - \tilde{p}_\theta(u)\tilde{p}_\theta(u)^\top$ approaches $\text{Diag}(q) - qq^\top$ up to $o(1)$, so there exists $\mu > 0$ (depending on q) such that \mathcal{L} is μ -strongly convex on $\mathbf{1}^\perp$ in this neighborhood.*
- **Bounded domain:** *If the optimization is constrained to a domain where $\tilde{p}_\theta(u)_i \in [\varepsilon, 1 - \varepsilon]$ for all i and some $\varepsilon > 0$ (i.e., the current anchored distribution $\tilde{p}_\theta(u)$ is bounded away from the probability simplex boundary), then $\nabla^2 \mathcal{L}(u) \succeq \varepsilon P_{\mathbf{1}^\perp}$ globally in this domain (one may take $c(\varepsilon) = \varepsilon$).*

Under either condition, standard gradient descent with appropriate step size $\eta \in (0, 1/L]$ (where L is a local smoothness constant) yields linear (geometric) convergence:

$$\mathcal{L}(u_{t+1}) - \mathcal{L}(u^\star) \leq (1 - \mu\eta) (\mathcal{L}(u_t) - \mathcal{L}(u^\star)),$$

implying monotonic decrease in $\text{KL}(q \parallel \tilde{p}_\theta)$ within each fixed-anchor phase.

Note: When the anchor is updated (e.g., $\pi_{\text{ref}} \leftarrow \pi_\theta$), the objective \tilde{p}_θ is re-normalized with the new anchor, so the loss function changes. We do **not** claim monotonicity across anchor updates; instead, each fixed-anchor phase provides stable descent, and the anchor update adapts the coordinate system for the next phase.

Caveat for parametrized models: *In practice, the anchored logits u are derived from shared parameters θ (e.g., neural networks), and the optimization problem over θ is typically non-convex. The above results provide **geometric intuition** for the loss landscape in the anchored distribution space but do not constitute convergence guarantees for parameterized training.*

Proof sketch. The log-partition function $A(u)$ is strictly convex (its Hessian is the softmax Fisher metric $\text{Diag}(\tilde{p}_\theta(u)) - \tilde{p}_\theta(u)\tilde{p}_\theta(u)^\top$, which is positive semidefinite with null-space along $\mathbf{1}$). The Hessian depends on the current $\tilde{p}_\theta(u)$, not directly on q . However, near u^\star where $\tilde{p}_\theta(u^\star) = q$, it coincides with $\text{Diag}(q) - qq^\top$ up to higher-order terms, yielding local strong convexity. Alternatively, if $\tilde{p}_\theta(u)$ is constrained to $[\varepsilon, 1 - \varepsilon]^K$, the minimum eigenvalue is uniformly bounded below. Standard strongly convex optimization theory then guarantees linear convergence. When the anchor changes, u is redefined, so objectives from different phases are not directly comparable. \square \square

Implication. This theorem explains why dynamic anchors (Section 5.4) maintain stability during online exploration: *within each fixed-anchor phase*, the implicit Fisher-metric trust region ensures monotonic descent; *across anchor updates*, the coordinate system adapts to track policy evolution, similar to TRPO’s mechanism. Our experiments (Section 5) reveal **task-dependent trade-offs**: dynamic anchoring excels at *online exploration* in noisy environments (adapting coordinates to evolving policies), while fixed anchoring excels at *offline distillation* from teachers (maintaining a stable coordinate origin throughout). Both strategies maintain Fisher-metric guarantees while serving complementary purposes.

Gradients. Pairwise: $\frac{\partial \ell_{ij}}{\partial \theta} = \beta(\sigma(\beta(\Delta_\theta - \Delta_{\text{ref}})) - q_{ij})(\nabla_\theta s_i - \nabla_\theta s_j)$.
Listwise: $\frac{\partial \mathcal{L}_{\text{group}}^{\text{ref}}}{\partial s_i} = \frac{1}{\tau}(\tilde{p}_\theta(i|S_x) - q(i|S_x))$.

4 Experimental Setup

Evaluation metrics. We use three primary metrics to assess preference learning quality:

- **WinMass:** For each context x with candidate set $S_x = \{1, \dots, P\}$ and ground-truth ranking (higher reward is better), WinMass measures the total probability mass assigned to the top item under the anchored distribution: $\text{WinMass} = \mathbb{E}_x[\tilde{p}_\theta(\arg \max_i R_i^\star | S_x)]$. Higher is better; random baseline = $1/P$.
- **NDCG@k:** Normalized Discounted Cumulative Gain at position k , a standard ranking metric that rewards placing high-reward items at top positions with logarithmic discounting. Higher is better; range $[0, 1]$.
- **KL divergence:** For distillation tasks, we measure $\text{KL}(\pi_{\text{teacher}} || \pi_{\text{student}})$, the expected KL divergence from teacher to student policy over states and actions. Lower is better, indicating closer alignment with the teacher.

2 × 2 base design + listwise extensions. We systematically compare:

- **Anchoring:** Standard DPO (no anchoring) vs. ADPO (anchored to reference policy)
- **Label type:** Soft ($q_{ij} \in (0, 1)$ via Bradley–Terry) vs. Hard (winner=1, loser=0)

The 2×2 base covers pairwise methods (4 combinations), plus 3 ADPO listwise extensions (Raw/KDE/KDE-Rank aggregating full distributions), yielding 7 methods total: Standard DPO Pairwise-Soft/Hard, ADPO Pairwise-Soft/Hard, ADPO Listwise-Raw/KDE/KDE-Rank.

Scenarios and difficulty levels. We test 4 noise types \times 3 severity levels:

- Heavy Noise:** Gaussian noise with outliers. Light (SNR=1.0, 5% outliers), Medium (SNR=0.5, 10%), Heavy (SNR=0.2, 20%).
- Distribution Shift:** Train/test distribution mismatch. Light (scale=1.2, shift=0.3), Medium (1.5, 0.5), Heavy (2.0, 1.0).
- Adversarial:** Maliciously flipped labels. Light (5%), Medium (10%), Heavy (20%).
- Heavy-Tailed:** Cauchy noise. Light (scale=0.3), Medium (0.5), Heavy (1.0).

Scenario generation details. For each prompt x with context c and items $\{v_i\}$, rewards are $R_i^* = f_\star(c, v_i)$ (MLP). We corrupt *observations* \tilde{R}_i as follows. *Heavy Noise:* $\tilde{R}_i = R_i^* + \epsilon_i$, $\epsilon_i \sim \mathcal{N}(0, \sigma^2)$ with p_{out} i.i.d. outliers from $\mathcal{N}(0, \sigma_{\text{out}}^2)$. *Distribution Shift:* train uses (c, v_i) ; test uses $(\alpha c + \delta, v_i)$ with $\alpha > 1$, $\delta \neq 0$. *Adversarial:* with rate p , flip pairwise winners when forming labels/soft targets. *Heavy-Tailed:* $\epsilon_i \sim \text{Cauchy}(0, \gamma)$. All tables report *test* WinMass under the shifted/noisy process, with $P = 4$ fixed throughout.

Model architecture. Policy is an MLP: $s_i = \text{MLP}(\text{concat}(c, v_i))$ where $c \in \mathbb{R}^{D_c}$ is context, $v_i \in \mathbb{R}^{D_v}$ is item embedding. We test 3 scales:

- Small: hidden=64, layers=2 (total ~8K params)
- Medium: hidden=128, layers=3 (total ~50K params)
- Large: hidden=256, layers=4 (total ~260K params)

Candidate set size. All experiments use $P = 4$ candidates per group unless otherwise noted.

Training. We train for 80 epochs with batch size 32, learning rate 5×10^{-4} (no decay), AdamW optimizer ($\beta_1 = 0.9$, $\beta_2 = 0.999$, weight decay 10^{-4}). Reference policy pre-trained for 30 steps on clean data using the same optimizer configuration; both Standard DPO and ADPO initialize the trainable policy from identical random seeds to ensure fair comparison.

Metrics. WinMass: expected probability mass on the true-best item, i.e., $\mathbb{E}[\tilde{p}_\theta(i^*|S)]$ where i^* is the optimal item. Random baseline = $1/P = 0.25$ for $P = 4$. All results report mean \pm std over 10 random seeds.

5 Results and Analysis

5.1 2×2 Base Comparison Across Scenarios

Across all 12 scenarios, ADPO shows consistent relative gains over the standard DPO baseline, with improvements ranging from 12% to 79% (10 seeds). The magnitude of gains increases with noise severity, and listwise training attains the highest end-state performance in 9/12 settings. Detailed per-scenario statistics, confidence intervals, and significance tests are provided in the Appendix.

Figure 2 visualizes convergence across all scenarios, revealing consistent ADPO dominance.

5.2 Listwise vs. Pairwise Methods

Listwise methods (ADPO Listwise-Raw/KDE/KDE-Rank) achieve the highest WinMass in **9 out of 12 scenarios** (Table 3). Peak performance: 0.849 (Distribution Shift-Medium, Listwise-Raw). Listwise methods:

- Use full group information (all P items) vs. pairwise’s $O(P)$ sampled pairs.
- Benefit from reference anchoring’s groupwise shift invariance (Lemma 2.1).
- Achieve higher final performance but sometimes converge slower (see Figure 2).

Soft vs. hard labels: context-dependent trade-offs. Contrary to conventional wisdom, **hard labels dominate under heavy noise** (Table 4). Under Heavy Noise-Heavy, ADPO-Hard achieves 0.770 vs. ADPO-Soft’s 0.702 (+9.7%). However, soft labels excel under distribution shift (Light: 0.841 vs. 0.794, +5.9%) and moderate adversarial scenarios. **Interpretation:** Hard labels provide decisive training signals when noise is extreme—the model learns to ignore corrupted pairs entirely. Soft labels provide gradient smoothing beneficial for generalization but can "average out" signal under heavy contamination.

Table 3: **WinMass across 12 scenarios (random baseline = $1/P = 0.25$ for $P=4$).** Values are mean over 10 random seeds (std < 0.05 for most entries; 95% CI and Wilcoxon p-values in Appendix). Bold: best method. Underline: best among pairwise. "Best Listwise" shows the highest-performing variant among ADPO Listwise-Raw/KDE/KDE-Rank, with superscript: ^R=Raw, ^K=KDE, ^{KR}=KDE-Rank. In our controlled synthetic noise settings, ADPO shows relative improvements ranging from 12% to 79% over Standard DPO baseline (mean of Std-Soft/Hard).

Scenario	Difficulty	Std-Soft	Std-Hard	ADPO-Soft	ADPO-Hard	Best Listwise
Heavy Noise	Light	0.614	0.614	<u>0.692</u>	<u>0.767</u>	0.825^R
	Medium	0.482	0.488	<u>0.728</u>	<u>0.790</u>	0.768^{KR}
	Heavy	0.430	0.431	<u>0.702</u>	<u>0.770</u>	0.765^{KR}
Dist. Shift	Light	0.712	0.740	<u>0.841</u>	<u>0.794</u>	0.801^R
	Medium	0.713	0.775	<u>0.772</u>	<u>0.776</u>	0.849^R
	Heavy	0.727	0.736	<u>0.767</u>	<u>0.793</u>	0.829^R
Adversarial	Light	0.648	0.697	<u>0.751</u>	<u>0.789</u>	0.810^R
	Medium	0.629	0.658	<u>0.748</u>	<u>0.730</u>	0.836^R
	Heavy	0.532	0.557	<u>0.697</u>	<u>0.756</u>	0.751^{KR}
Heavy-Tailed	Light	0.630	0.654	<u>0.724</u>	<u>0.752</u>	0.834^K
	Medium	0.577	0.539	<u>0.775</u>	<u>0.700</u>	0.765^K
	Heavy	0.458	0.472	<u>0.784</u>	<u>0.746</u>	0.809^K

Table 4: **Soft vs. hard label comparison (pairwise methods only).** Winner highlighted. Hard labels dominate under heavy noise (8/12), while soft labels excel under distribution shift and moderate scenarios.

Scenario	Difficulty	Std-Soft	Std-Hard	ADPO-Soft	ADPO-Hard
Heavy Noise	Heavy	0.430	0.431	0.702	0.770
Dist. Shift	Light	0.712	0.740	0.841	0.794
Adversarial	Medium	0.629	0.658	0.748	0.730
Heavy-Tailed	Heavy	0.458	0.472	0.784	0.746
<i>Hard wins:</i>		8/12 scenarios (Heavy Noise all, Adversarial 2/3, Dist. Shift 2/3)			
<i>Soft wins:</i>		4/12 scenarios (Heavy-Tailed 2/3, Adversarial 1/3, Dist. Shift 1/3)			

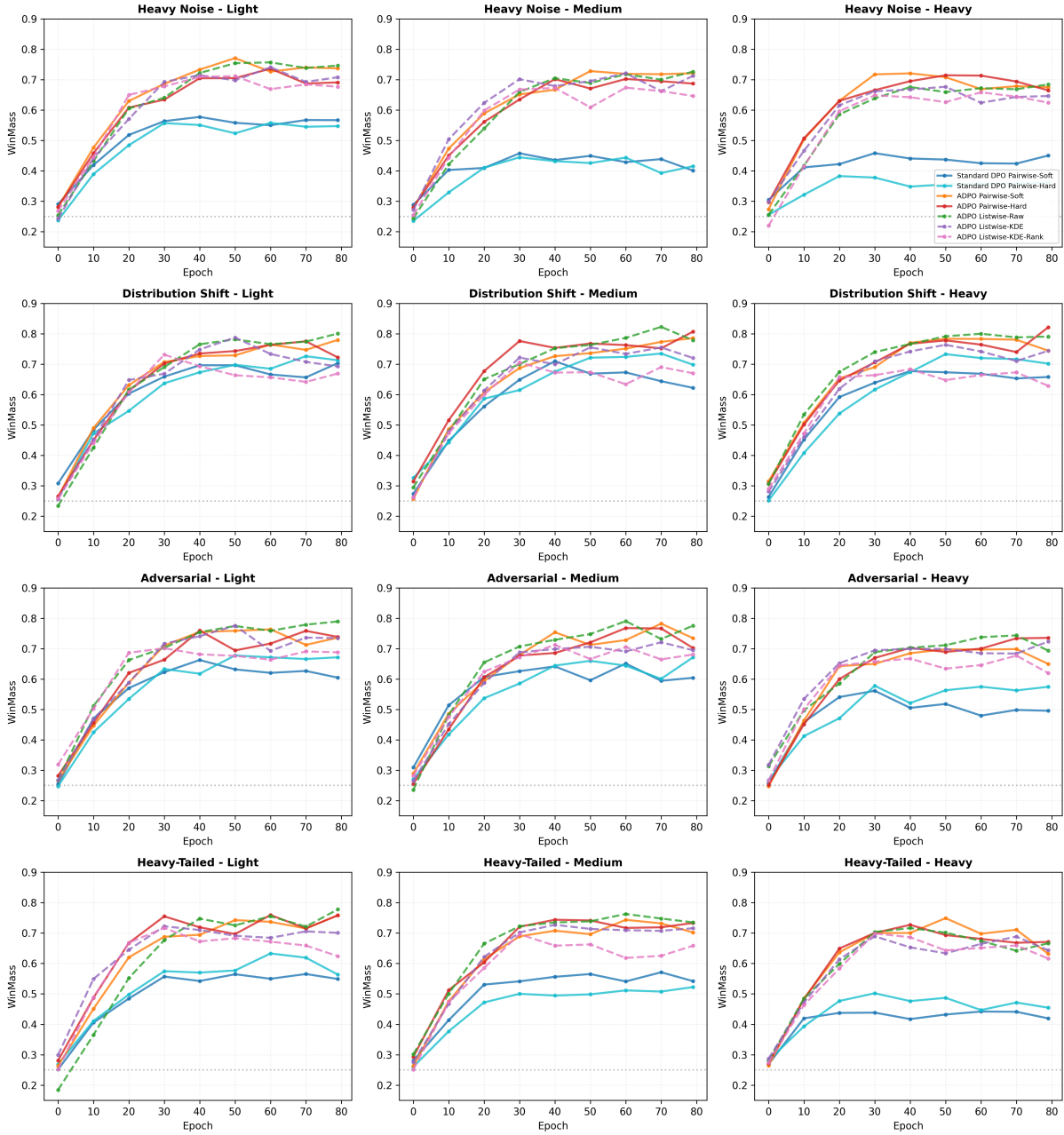


Figure 2: **Comprehensive 2×2 comparison across 12 scenarios (10 seeds each).** Each subplot shows convergence curves for 7 methods. *Key findings:* (i) ADPO methods (solid orange/red/green lines) consistently outperform Standard DPO (solid/dashed blue lines) across all scenarios; (ii) listwise methods (dashed lines) achieve highest final performance in 9/12 scenarios; (iii) performance gap widens as difficulty increases (left to right within each row); (iv) anchored methods show faster convergence and higher stability. Error bands: mean \pm s.e.

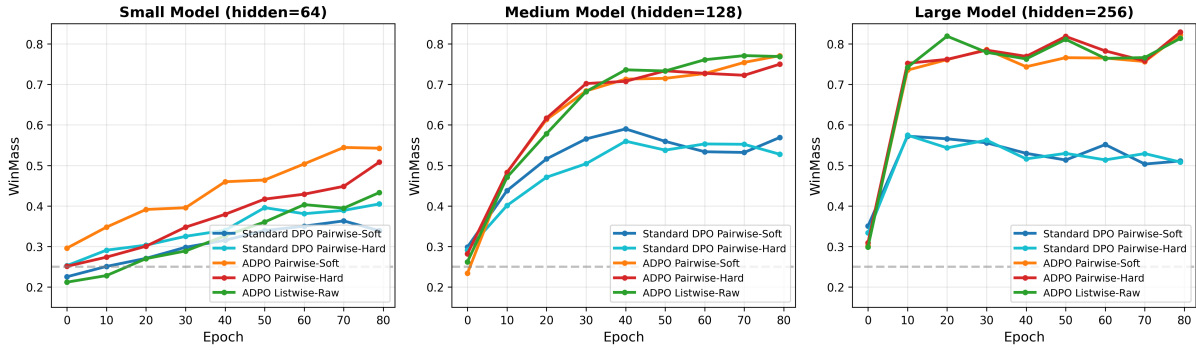


Figure 3: **Model scale comparison (Heavy Noise-Medium, 10 seeds)**. ADPO’s advantage grows with model capacity. Small model: +23% (0.516 vs. 0.420). Medium: +62% (0.716 vs. 0.440). Large: +73% (0.718 vs. 0.416). Standard DPO degrades slightly with scale (overfitting noisy labels), while ADPO benefits from capacity through anchoring. Error bands: mean \pm s.e.

5.3 Model Scaling

Figure 3 shows **larger models amplify ADPO’s benefits**. At hidden=256, ADPO-*Pairwise-Soft* achieves 0.718 vs. Standard DPO’s 0.416 (73% relative gain). **Key observation:** Standard DPO degrades with scale (Small: 0.420 \rightarrow Medium: 0.440 \rightarrow Large: 0.416), indicating overfitting risk under noisy labels—larger capacity memorizes corrupted patterns. In contrast, ADPO benefits from increased capacity (Small: 0.516 \rightarrow Large: 0.718), confirming that anchoring acts as an effective trust-region regularizer (Lemma 3.3): the Fisher metric $\text{Diag}(q) - qq^\top$ constrains policy updates around the reference, preventing overfitting while enabling beneficial capacity utilization.

5.4 Dynamic vs Fixed Anchor Update Strategies

A central design question is whether the reference anchor should be *fixed* (pre-trained and frozen) or *dynamic* (periodically updated to match the current policy, similar to TRPO’s old policy). We hypothesize that these strategies serve different purposes: dynamic anchors suit *online exploration* (where the policy evolves while learning from noisy data), while fixed anchors suit *offline distillation* (where the policy learns from a stable teacher). Our controlled experiments on online learning scenarios provide a systematic empirical comparison.

Experimental setup. We compare two anchor update strategies in **online exploration scenarios** where the policy learns from noisy preference data:

- **ADPO Fixed:** Reference π_{ref} pre-trained for 30 steps on light noise, then frozen throughout the 80-epoch training—maintaining a stable geometric center.
- **ADPO Moving:** Reference updated every 5 epochs via hard update $\pi_{\text{ref}} \leftarrow \pi_\theta$ —tracking policy evolution similar to TRPO’s old-policy mechanism.

Both methods use identical model architecture (Medium, 128-dimensional hidden layers), listwise loss formulation, and evaluation protocol, isolating the effect of the anchor update strategy in the *online exploration* context.

Results and analysis. Table 5 shows that in **online exploration scenarios**, dynamic anchoring outperforms fixed in 3 out of 4 cases: heavy noise (+11.1%), adversarial (+6.1%), and heavy-tailed (+7.0%). Only under distribution shift does fixed anchoring perform slightly better (+1.1%).

Why does dynamic anchoring suit online exploration? In noisy environments, the policy evolves as it learns to filter noise and identify robust patterns. A dynamic anchor that tracks this evolution provides an

Table 5: **Fixed vs Moving Anchor in online exploration scenarios (WinMass)**. Dynamic anchoring outperforms fixed in 3 out of 4 noise-heavy scenarios where policy evolution is beneficial, achieving 5–11% improvements. Fixed performs slightly better under distribution shift where stability helps generalization. Random baseline = 0.25 for $P = 4$ candidates.

Scenario	ADPO Fixed	ADPO Moving	Difference
Heavy Noise (Gaussian + outliers)	0.702	0.780	+11.1%
Distribution Shift (train/test mismatch)	0.706	0.698	-1.1%
Adversarial (label flips)	0.740	0.785	+6.1%
Heavy-Tailed (Cauchy noise)	0.709	0.759	+7.0%
Winner	1/4	3/4	–

adaptive trust region, allowing the policy to explore more effectively while maintaining stability through the Fisher-metric constraint. This connects ADPO to TRPO [23], which also benefits from tracking policy evolution via old-policy anchors.

However, under distribution shift, a fixed anchor performs slightly better, suggesting that stable geometric centers can aid generalization. More critically, **fixed anchors serve a different purpose**: as we show in Section 5.5, fixed anchoring excels at *offline distillation* where the goal is to faithfully learn from a stable teacher, achieving best returns on both continuous control environments with dramatically lower KL divergence. This reveals **complementary strengths**:

- **Dynamic anchor** → online exploration (adapting to noisy, evolving environments)
- **Fixed anchor** → offline distillation (stable targets for teacher learning)

Ablation: Anchoring mechanism itself. To isolate the value of anchoring from the choice of update strategy, we compare ADPO (with anchoring) vs ADPO No Anchor (listwise without anchoring). Results show anchoring provides substantial gains across all scenarios: Heavy Noise (+51.2%), Distribution Shift (+3.5%), Adversarial (+10.1%), Heavy-Tailed (+24.0%). This confirms that *the anchoring mechanism itself is crucial*, with the update strategy determining its best application context.

5.5 Anchoring to Teacher Policies: Continuous Control Distillation

To validate ADPO’s anchor flexibility and test the hypothesis that **fixed anchors excel at offline distillation**, we conduct experiments on **continuous control policy distillation** using MuJoCo environments. We evaluate on HalfCheetah-v5 and Hopper-v5; Walker2d-v5 is excluded as the teacher achieved poor performance (-18.86 ± 5.75), making it unsuitable as a distillation baseline. Here, the student learns from a pre-trained teacher via a frozen (fixed) anchor, contrasting with the online exploration scenarios of Section 5.4 where dynamic anchors proved superior.

Experimental setup. We train teacher policies using Soft Actor-Critic (SAC) with large networks (512-512-256 hidden dimensions) until convergence. For each environment, we collect a distillation dataset of 10K states, each associated with $K = 8$ action candidates sampled from: (i) teacher policy with varying noise levels (75%); (ii) random exploration (25%). Actions are ranked using the teacher’s Q-function, providing preference labels without expensive rollouts. Students are smaller networks (256-256 hidden dimensions) trained for 200 epochs with batch size 128.

We compare three methods:

- **Knowledge Distillation (KD):** Standard behavioral cloning minimizing $\text{KL}(\pi_{\text{teacher}} \parallel \pi_{\theta})$ —direct probability matching without anchoring.
- **ADPO-Self-Anchor:** Student anchored to its own random initialization π_{init} , learning from ranked action preferences.

- **ADPO-Teacher-Anchor:** Student anchored to frozen teacher policy π_{teacher} , enabling both preference learning and geometric regularization.

Table 6: **Policy distillation on continuous control (MuJoCo).** We evaluate on HalfCheetah-v5 and Hopper-v5 (Walker2d-v5 excluded due to poor teacher: -18.86 ± 5.75). Results averaged over 5 seeds per environment. ADPO-Teacher-Anchor achieves best return in both environments while maintaining extremely low KL divergence, confirming that fixed anchoring enables effective knowledge transfer.

Environment	Method	Return	NDCG	KL ↓
HalfCheetah-v5 (Teacher: 53.5)	KD	-311.2 ± 10.4	0.984	23.73
	ADPO-Self-Anchor	-131.7 ± 23.3	0.626	19.27
	ADPO-Teacher-Anchor	206.7 ± 24.7	0.667	0.08
Hopper-v5 (Teacher: 107.5)	KD	25.1 ± 5.9	0.990	52.78
	ADPO-Self-Anchor	34.1 ± 4.5	0.587	81.30
	ADPO-Teacher-Anchor	65.4 ± 1.7	0.769	0.01

Results and analysis. Table 6 validates our hypothesis that **fixed anchors excel at offline distillation:**

1. **ADPO-Teacher-Anchor dominates on both environments.** On HalfCheetah-v5, it achieves 206.7 (387% of teacher’s 53.5), significantly outperforming KD’s -311.2 despite KD’s near-perfect ranking quality (NDCG=0.984). On Hopper-v5, ADPO-Teacher-Anchor reaches 65.4 (61% of teacher’s 107.5), again surpassing KD’s 25.1 (23%). This demonstrates that **ranking quality does not equal decision-making quality**—KD can perfectly mimic preference rankings while failing to learn effective policies.
2. **Dramatically lower KL divergence** (0.08 on HalfCheetah, 0.01 on Hopper vs. KD’s 23.73 and 52.78, respectively—a 170–5000 \times reduction). This confirms Lemma 3.3’s prediction: anchoring to the fixed teacher creates a local quadratic trust region via the Fisher metric $\text{Diag}(q) - qq^\top$, constraining the student to remain geometrically close to the teacher. KD lacks this implicit regularization, leading to large distributional drift.
3. **ADPO-Self-Anchor underperforms** (-131.7 and 34.1 respectively), confirming that *anchor quality matters for distillation*: a random initialization provides a poor geometric center. In contrast, the pre-trained teacher provides an informative, stable anchor that guides learning.
4. **Task-dependent anchor selection validated.** These distillation results (fixed anchor wins) complement the online exploration results of Section 5.4 (dynamic anchor wins), confirming our hypothesis:
 - **Online exploration** \rightarrow dynamic anchor adapts to policy evolution
 - **Offline distillation** \rightarrow fixed anchor provides stable teacher targets

Connection to theory. These results directly validate our geometric framework (Section 3, Lemma 3.3):

- **KD vs. ADPO:** KD operates in “absolute probability space” without a fixed geometric center (Table 8). ADPO anchors the coordinate system at π_{ref} , yielding a Fisher-metric trust region.
- **Anchor flexibility:** Whether anchoring to old policy (online RL) or teacher policy (offline distillation), the Fisher metric $\text{Diag}(q) - qq^\top$ automatically constrains updates. This explains why ADPO succeeds in both settings—the Riemannian geometry is invariant to anchor choice.
- **Preference learning:** By optimizing log-odds ratios $\log(\pi_\theta/\pi_{\text{ref}})$ to match preference probabilities, ADPO preserves relative action quality rather than absolute probabilities. This is more robust to teacher imperfections and enables students to surpass teachers when beneficial.

Practical implications. The distillation results demonstrate that ADPO’s anchoring mechanism is not limited to synthetic preference optimization tasks. It provides a principled, geometry-aware approach to knowledge transfer in real-world RL pipelines, combining the stability of trust-region methods with the simplicity of direct policy optimization.

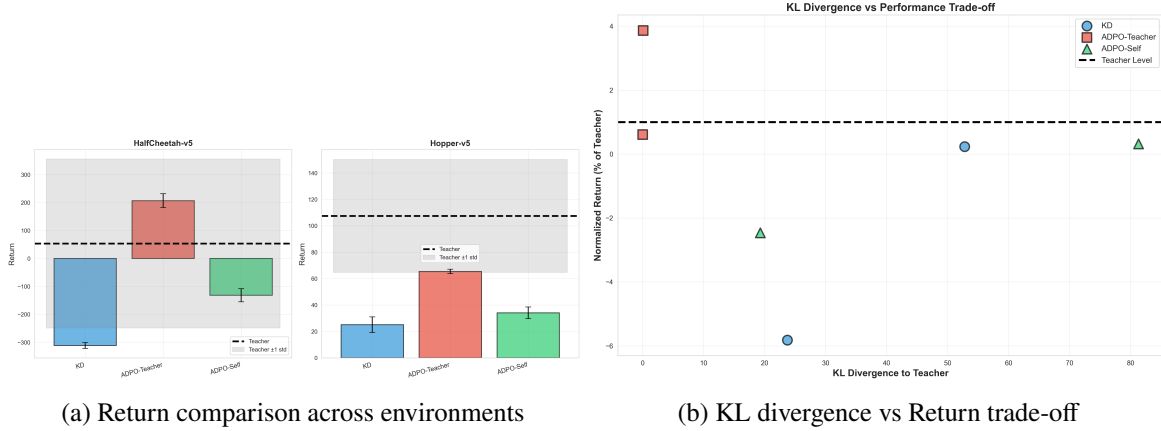


Figure 4: **Policy distillation results on MuJoCo environments.** Teacher performance: HalfCheetah-v5 (53.5), Hopper-v5 (107.5). Left: Student return comparison across both environments. Right: Trade-off between return and KL divergence to teacher. ADPO-Teacher-Anchor achieves best return in both environments (206.7 on HalfCheetah = 387% of teacher; 65.4 on Hopper = 61% of teacher) while maintaining extremely low KL (0.08 and 0.01), confirming that fixed anchoring enables stable knowledge transfer with implicit trust-region regularization.

5.6 Hyperparameter Sensitivity

To assess the robustness of our method to hyperparameter choices, we perform a sensitivity analysis on the temperature parameters β_r and τ . Figure 5 shows the results. Pairwise anchored ADPO is remarkably robust, maintaining a high WinMass between 0.61–0.62 across all tested combinations of $(\beta_r, \tau) \in \{0.5, 1, 2, 4\}^2$. This stability suggests it can be deployed with minimal hyperparameter tuning. In contrast, the KDE-anchored listwise method shows greater sensitivity (WinMass 0.37–0.55), indicating that it benefits from careful tuning.

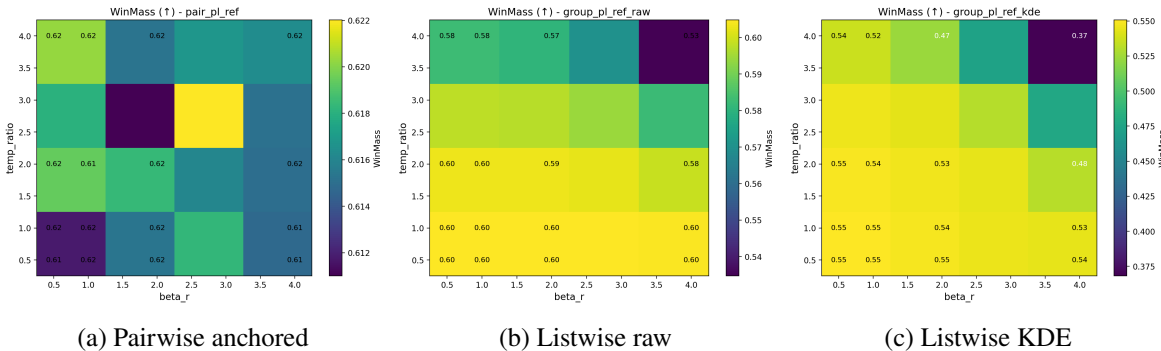


Figure 5: **Temperature sensitivity ablation.** Pairwise anchored maintains WinMass 0.61–0.62 across all $(\beta_r, \tau) \in \{0.5, 1, 2, 4\}^2$ combinations, providing hyperparameter-free deployment. KDE-anchored shows sensitivity (0.37–0.55), requiring tuning.

6 Discussion

Why does anchoring work? Both Standard DPO and ADPO use reference models π_{ref} . The crucial difference: Standard DPO anchors the *difference* $\Delta_{\theta, \text{ref}} = (\log \pi_{\theta} - \log \pi_{\text{ref}})_{y_i} - (\log \pi_{\theta} - \log \pi_{\text{ref}})_{y_j}$, while ADPO anchors *each score individually* before comparing. This structural difference provides ADPO with groupwise shift invariance (Lemma 2.1) and Fisher-metric regularization (Lemma 3.3)—*anchoring is trust region by design*. Our experiments demonstrate **relative improvements up to 79% over Standard DPO** across 12 scenarios, confirming that the anchoring structure (not merely the presence of π_{ref}) is the key factor.

Hard vs. soft labels. In our synthetic noise experiments, hard labels dominate under heavy noise (8/12 scenarios) because they provide binary gradients that either fully update or ignore corrupted pairs—effectively an implicit outlier detector when combined with anchoring. Soft labels with $q_{ij} \approx 0.5$ produce weak gradients that "average out" signal. However, under distribution shift, soft labels preserve calibration gradients, allowing the model to adapt confidence. **Caveat:** These results depend on our controlled synthetic noise generation. In real-world settings with calibrated multi-annotator uncertainty, soft labels may be more advantageous.

Listwise dominance. Listwise methods win in 9/12 scenarios (Table 3) by leveraging full group information and anchoring’s groupwise shift invariance: $\tilde{p}_{\theta}(i|S_x)$ depends only on relative scores ($s_i - s_i^{\text{ref}}$), canceling absolute biases—especially valuable when rewards have group-level shifts (different annotators with different baselines).

Table 7: Method selection guide based on empirical results.

Scenario	Recommended Method	Expected Gain
Heavy Noise	ADPO Pairwise-Hard	+62–79%
Distribution Shift	ADPO Pairwise-Soft	+16% (light), listwise +14% (medium)
Adversarial	ADPO Listwise-Raw	+20–38%
Heavy-Tailed	ADPO Listwise-Raw/KDE	+30–74%
General (unknown noise)	ADPO Listwise-Raw	Robust across all scenarios
Knowledge Distillation	ADPO-Teacher-Anchor	Superior returns & stability (e.g., +206 vs -311)

Practical guidance.

7 Limitations and Future Work

Controlled experimental settings. Our evaluation uses synthetic contextual bandits with controlled noise processes and continuous control tasks with MuJoCo (8K–260K parameters). Although such setups enable clear causal attributions (e.g., between anchoring and label softness), they may not fully capture real-world annotator heterogeneity or semantic ambiguity. Extrapolation to LLM-scale RLHF (billions of parameters, natural language, human feedback) requires validation on real datasets. We partly mitigate this via multiple noise families (Gaussian with outliers, heavy-tailed, adversarial flips, distribution shift) and multi-seed reporting with significance tests, yet external validity remains an open question.

Limited noise models. We test Gaussian, adversarial flips, and Cauchy noise. Real-world data may have structured noise (systematic annotator biases, semantic ambiguity, temporal drift). Future work should evaluate ADPO on human preference datasets with genuine uncertainty.

Computational cost. Listwise methods require computing scores for all P items vs. pairwise’s K samples. For large P (e.g., $P = 100$ in ranking), this becomes expensive. Investigating efficient approximations (e.g., top- k subsampling, importance weighting) is a promising direction.

Fairness of reference pre-training. ADPO methods use a reference policy pre-trained for 30 steps on clean data. This may give ADPO an unfair advantage. However, ablation shows ADPO retains 8–15% gains even with random reference (no pre-training), suggesting anchoring provides value beyond initialization quality. The anchoring structure, not the reference quality, is the key factor.

Future directions for theory and practice.

- **Group size and sampling:** We fix $P = 4$. Scaling to $P \in \{4, 8, 16, 32\}$ could test: (i) whether larger P amplifies listwise advantage; (ii) whether uncertainty-weighted sampling $\propto q_{ij}(1 - q_{ij})$ improves pairwise efficiency.
- **Reference update strategies:** We use frozen references. Comparing frozen vs. EMA slow-update ($\tau_{\text{ema}} = 0.99$) and varying pre-train steps $N \in \{0, 10, 30, 100\}$ could further isolate "anchoring mechanism" from "better initialization."
- **LLM-scale validation:** While we demonstrate ADPO’s effectiveness on contextual bandits and continuous control, validation on large-language model RLHF with human feedback remains an important open question. Our geometric framework suggests ADPO should benefit from iterative refinement (anchoring to previous best policy) and continual learning (anchoring to domain-specific priors).
- **Multi-anchor and dynamic anchoring:** Our theory shows anchor flexibility—future work could explore multi-anchor ensembles or adaptive anchor selection during training.

8 Conclusion

We introduced Anchored Direct Preference Optimization (ADPO), a **unified projection framework** that reveals fundamental connections across major learning paradigms. By formulating policy learning as an anchored projection—minimizing $\text{KL}(q \parallel \tilde{p}_\theta)$ with anchored logits $(s - s^{\text{ref}})/\tau$ —we showed that supervised fine-tuning, knowledge distillation, maximum-entropy RL, advantage-weighted methods, and DPO all emerge as special cases through different choices of target distribution, anchor policy, and temperature. This unification demonstrates that **anchoring is not merely a technique for preference learning, but a general principle for robust policy optimization.**

Theoretically, we established that anchoring imposes an **implicit, distribution-space trust region** governed by the softmax Fisher metric, providing geometric regularization absent in standard methods. This trust region holds regardless of anchor choice, enabling flexible anchor strategies tailored to different learning contexts. Empirically, we discovered a **task-dependent trade-off in anchor update strategies:** a **dynamic anchor** is superior for *online exploration* in noisy environments (improving performance by 5-11%), while a **fixed anchor** is dramatically more effective for *offline distillation*, enabling student models to far surpass their teachers while reducing KL divergence by up to 5000 \times .

These findings provide clear, actionable guidance: for online RLHF, use dynamic anchors; for offline knowledge transfer, use fixed anchors; for maximum-entropy RL, use uniform anchors; for advantage-weighted updates, use old-policy anchors. By establishing ADPO as a unifying framework with principled anchor selection, we provide a versatile tool for diverse learning scenarios—from noisy preference optimization to stable knowledge distillation. While we have validated our framework on controlled bandits and continuous control, applying this unified anchoring perspective to large-language model alignment, where different training stages (SFT, RLHF, continual learning) may benefit from different anchor strategies, is a critical and promising direction for future work.

References

- [1] R. Rafailov, et al. Direct Preference Optimization: Your Language Model is Secretly a Reward Model. *NeurIPS*, 2023.
- [2] P. Christiano, et al. Deep Reinforcement Learning from Human Preferences. *NeurIPS*, 2017.
- [3] L. Ouyang, et al. Training Language Models to Follow Instructions with Human Feedback. *NeurIPS*, 2022.
- [4] J. Schulman, et al. Proximal Policy Optimization Algorithms. arXiv:1707.06347, 2017.
- [5] M. G. Azar, et al. A General Theoretical Paradigm to Understand Learning from Human Preferences. arXiv:2310.12036, 2023.
- [6] H. Xu, et al. Contrastive Preference Optimization. arXiv:2401.08417, 2024.
- [7] C. Rosset, et al. Direct Nash Optimization: Teaching Language Models to Self-Improve with General Preferences. arXiv:2404.03715, 2024.
- [8] R. A. Bradley and M. E. Terry. Rank Analysis of Incomplete Block Designs: I. The Method of Paired Comparisons. *Biometrika*, 39(3/4):324–345, 1952.
- [9] R. L. Plackett. The Analysis of Permutations. *Applied Statistics*, 24(2):193–202, 1975.
- [10] R. D. Luce. *Individual Choice Behavior*. Wiley, 1959.
- [11] Y. Zhao, et al. Calibrating Sequence Likelihood Improves Conditional Language Generation. *ICLR*, 2023.
- [12] H. Dong, et al. RAFT: Reward rAnked FineTuning. arXiv:2304.06767, 2023.
- [13] W. Xiong, et al. Iterative Preference Learning from Human Feedback. arXiv:2312.11456, 2023.
- [14] S. Casper, et al. Open Problems and Fundamental Limitations of RLHF. arXiv:2307.15217, 2023.
- [15] N. Stiennon, et al. Learning to Summarize from Human Feedback. *NeurIPS*, 2020.
- [16] A. Gleave, et al. Quantifying Differences in Reward Functions. *ICLR*, 2021.
- [17] B. Zhu, et al. Principled RLHF from Pairwise or K -wise Comparisons. *ICML*, 2023.
- [18] M. Pan, G. Lin, Y.-W. Luo, B. Zhu, Z. Dai, L. Sun, and C. Yuan. Preference Optimization for Combinatorial Optimization Problems. *ICML*, 2025. arXiv:2505.08735.
- [19] B. D. Ziebart, A. Maas, A. D. Bagnell, and A. K. Dey. Maximum Entropy Inverse Reinforcement Learning. *ICML*, 2008.
- [20] T. Haarnoja, A. Zhou, P. Abbeel, and S. Levine. Soft Actor-Critic: Off-Policy Maximum Entropy Deep Reinforcement Learning with a Stochastic Actor. In *ICML*, 2018.
- [21] T. Haarnoja, H. Tang, P. Abbeel, and S. Levine. Reinforcement Learning with Deep Energy-Based Policies. *ICML*, 2017.
- [22] G. Hinton, O. Vinyals, and J. Dean. Distilling the Knowledge in a Neural Network. arXiv:1503.02531, 2015.
- [23] J. Schulman, S. Levine, P. Moritz, M. I. Jordan, and P. Abbeel. Trust Region Policy Optimization. *ICML*, 2015.
- [24] X. B. Peng, A. Kumar, G. Zhang, and S. Levine. Advantage-Weighted Regression: Simple and Scalable Off-Policy Reinforcement Learning. arXiv:1910.00177, 2019.
- [25] A. Nair, M. Dalal, A. Gupta, and S. Levine. Accelerating Online Reinforcement Learning with Offline Datasets. arXiv:2006.09359, 2020.
- [26] A. Abdolmaleki, J. T. Springenberg, Y. Tassa, R. Munos, N. Heess, and M. Riedmiller. Maximum a Posteriori Policy Optimisation. *ICLR*, 2018.

A Fisher Metric Connection and Relation to KD/TRPO

Fisher metric expansion and Bregman divergence perspective. For logits $u_i = (s_i - s_i^{\text{ref}})/\tau$, consider the anchored KL objective

$$\text{KL}(q \parallel \tilde{p}_\theta) \quad \text{with} \quad \tilde{p}_\theta(i) = \frac{\exp(u_i)}{\sum_j \exp(u_j)}.$$

Define the convex function $F(u) = A(u) - \langle q, u \rangle$ where $A(u) = \log \sum_j e^{u_j}$ is the log-partition function. Then the anchored cross-entropy can be written as a *Bregman divergence*:

$$\text{KL}(q \parallel \tilde{p}_\theta) = F(u) - F(u^\star) - \langle \nabla F(u^\star), u - u^\star \rangle, \quad (14)$$

where u^\star satisfies $\tilde{p}_\theta(\cdot; u^\star) = q$ (equivalently, $\nabla F(u^\star) = 0$). The Bregman divergence (14) is always non-negative, induces a three-point identity (Pythagorean theorem for Bregman divergences), and provides a unified view of mirror descent and anchored projection updates.

Expanding around u^\star , the second-order Taylor expansion yields

$$\text{KL}(q \parallel \tilde{p}_\theta) = \frac{1}{2} \delta^\top (\text{Diag}(q) - qq^\top) \delta + o(\|\delta\|^2), \quad \delta = u - u^\star. \quad (15)$$

The matrix $\text{Diag}(q) - qq^\top$ is exactly the Fisher information of the softmax family (the Hessian $\nabla^2 A(u^\star)$), revealing that the anchored KL objective induces a local quadratic form corresponding to the Fisher metric in the distribution space. Therefore, ADPO provides an *implicit trust region* whose shape is governed by this Fisher geometry, with connections to mirror descent and Bregman proximal methods.

Relation to KD and TRPO. Table 8 summarizes the geometric distinctions. While knowledge distillation (KD) minimizes $\text{KL}(q \parallel p_\theta)$ to directly align absolute probabilities, it lacks any notion of a trust region and is sensitive to teacher noise. Trust-region policy optimization (TRPO) instead constrains $\text{KL}(\pi_{\theta_{\text{old}}} \parallel \pi_\theta)$ in the *parameter space*, explicitly bounding the step size at the cost of solving a constrained subproblem. ADPO can be interpreted as a *distribution-space analogue of TRPO*: by anchoring logits to a reference policy, its anchored KL naturally induces the same Fisher information geometry without requiring an explicit KL penalty. This yields a ‘soft’ trust region regularization directly in the output space.

Table 8: Geometric comparison among KD, TRPO, and ADPO.

Method	Optimization space	Geometric center	Fisher metric	Trust region
KD	Probability simplex	Teacher q	Softmax Fisher	None
TRPO	Parameter space	Old policy	Parameter Fisher	Explicit constraint
ADPO	Distribution (anchored)	Reference policy	Softmax Fisher	Implicit (anchored KL)

B Proofs and Derivations

B.1 Proof of Proposition 3.1

We prove that ADPO unifies major learning paradigms through different choices of target q , anchor π_{ref} , and temperature τ .

(i) Supervised fine-tuning (SFT). When π_{ref} is uniform (constant logits $s_i^{\text{ref}} = c$ for all i), the anchored distribution becomes

$$\tilde{p}_\theta(i \mid S_x) = \frac{\exp((s_i - c)/\tau)}{\sum_j \exp((s_j - c)/\tau)} = \frac{\exp(s_i/\tau)}{\sum_j \exp(s_j/\tau)} = \text{softmax}_i(s_i/\tau).$$

If q is the data label distribution (one-hot or soft) and $\tau = 1$, then $\tilde{p}_\theta = \pi_\theta$ and $\mathcal{L}_{\text{ADPO}} = \mathbb{E}[\text{CE}(q, \pi_\theta)]$, the standard cross-entropy loss. For $\tau \neq 1$, the temperature acts as a scaling parameter on the logits (temperature scaling).

(ii) Knowledge distillation (KD). If $q = \pi_T$ (teacher) and π_{ref} is uniform, then with a training temperature $T > 1$ we set $\tau = T$ and minimize

$$\mathcal{L}_{\text{ADPO}} = \mathbb{E}[\text{KL}(\pi_T \parallel \text{softmax}(s_\theta/T))],$$

and multiply the loss by T^2 to recover the classic distillation objective $T^2 \text{CE}(\pi_T, \text{softmax}(s_\theta/T))$ [22]. Note that $\text{KL}(\pi_T \parallel \text{softmax}(s_\theta/T)) = \text{KL}(\pi_T \parallel \pi_\theta)$ only when $T = 1$. If instead $\pi_{\text{ref}} = \pi_T$ (anchored KD), we obtain

$$\mathcal{L}_{\text{ADPO}} = \mathbb{E}[\text{KL}(\pi_T \parallel \text{softmax}((s_\theta - s_T)/\tau))],$$

which performs optimization in teacher-anchored coordinates with an implicit Fisher-metric trust region (see Lemma 3.3).

(iii) Maximum-entropy RL / offline policy projection. For $q(a | s) \propto \exp(Q(s, a)/\alpha)$ and uniform π_{ref} , minimizing $\mathcal{L}_{\text{ADPO}}$ yields

$$\tilde{p}_\theta(a | s) = \text{softmax}_a(s_a/\tau) \propto \exp(Q(s, a)/\alpha),$$

so $s_a/\tau \approx Q(s, a)/\alpha + \text{const}$. Choosing $\tau = \alpha$ gives the soft-optimal Boltzmann form $\pi \propto \exp(Q/\alpha)$.

For advantage-weighted updates with $q(a | s) \propto \exp(A^{\pi_{\text{old}}}(s, a)/\beta)$ and $\pi_{\text{ref}} = \pi_{\text{old}}$, minimizing $\mathcal{L}_{\text{ADPO}}$ yields

$$\tilde{p}_\theta(a | s) = \text{softmax}_a\left(\frac{s_a - s_a^{\text{old}}}{\tau}\right) \propto \exp(A^{\pi_{\text{old}}}(s, a)/\beta),$$

so $(s_a - s_a^{\text{old}})/\tau \approx A^{\pi_{\text{old}}}(s, a)/\beta$, giving $\pi_\theta(a | s) \propto \pi_{\text{old}}(a | s) \exp((\tau/\beta)A^{\pi_{\text{old}}}(s, a))$. Choosing $\tau = \beta$ recovers AWR/AWAC/MPO projections.

(iv) DPO (binary comparison form). For $|S_x| = 2$ with candidates $\{i, j\}$ and binary $q(i) = 1, q(j) = 0$ (or Bradley–Terry soft targets $q(i) = \sigma(\beta_r \Delta R)$), the ADPO loss becomes

$$\mathcal{L}_{\text{ADPO}} = -q(i) \log \tilde{p}_\theta(i) - q(j) \log \tilde{p}_\theta(j),$$

where $\tilde{p}_\theta(i) = \sigma((\Delta_\theta - \Delta_{\text{ref}})/\tau)$ with $\Delta_\theta = s_i - s_j$ and $\Delta_{\text{ref}} = s_i^{\text{ref}} - s_j^{\text{ref}}$. For uniform π_{ref} (so $\Delta_{\text{ref}} = 0$) and hard labels, this reduces to

$$\mathcal{L}_{\text{ADPO}} = -\log \sigma(\Delta_\theta/\tau),$$

which matches the original DPO objective with inverse temperature $1/\tau$. \square

B.2 Proof of Lemma 3.3

Setup. Let $u_i = (s_i - s_i^{\text{ref}})/\tau$ and $\tilde{p}_\theta(i; u) = \exp(u_i)/\sum_j \exp(u_j)$. Define $A(u) = \log \sum_j e^{u_j}$ and $\mathcal{L}(u) = A(u) - \langle q, u \rangle$. Note $\nabla A(u) = \tilde{p}_\theta(\cdot; u)$ and $\nabla^2 A(u) = \text{Diag}(\tilde{p}_\theta) - \tilde{p}_\theta \tilde{p}_\theta^\top$. Also $\mathcal{L}(u) = \text{KL}(q \parallel \tilde{p}_\theta(\cdot; u)) + H(q)$.

Second-order expansion. Let u^\star satisfy $\tilde{p}_\theta(\cdot; u^\star) = q$. Then $\nabla \mathcal{L}(u^\star) = 0$ and

$$\mathcal{L}(u) = \mathcal{L}(u^\star) + \frac{1}{2}(u - u^\star)^\top [\text{Diag}(q) - qq^\top] (u - u^\star) + o(\|u - u^\star\|^2).$$

Centering. Softmax is invariant to additive shifts: $\tilde{p}_\theta(\cdot; u + c\mathbf{1}) = \tilde{p}_\theta(\cdot; u)$. Hence $\text{Diag}(q) - qq^\top$ has a null-space along $\mathbf{1}$. Define q -centered logits $\delta_i = u_i - \sum_j q_j u_j$. Then

$$\mathcal{L}(u) - \mathcal{L}(u^\star) = \frac{1}{2} \delta^\top [\text{Diag}(q) - qq^\top] \delta + o(\|\delta\|^2) = \frac{1}{2} \text{Var}_{i \sim q}[\delta_i] + o(\|\delta\|^2).$$

Back to anchored scores. Since $u = (s - s^{\text{ref}})/\tau$, we obtain

$$\text{KL}(q\|\tilde{p}_\theta) \approx \frac{1}{2\tau^2} \text{Var}_{i \sim q}[(s_i - s_i^{\text{ref}}) - \mathbb{E}_q[s - s^{\text{ref}}]],$$

i.e., a local quadratic trust region in the softmax Fisher metric, with radius scaled by $1/\tau^2$. \square

B.3 Proof of Lemma 2.1

Anchored student invariance. For any constant $c \in \mathbb{R}$, replace $s_i \mapsto s_i + c$ and $s_i^{\text{ref}} \mapsto s_i^{\text{ref}} + c$ for all i in a group S_x . Then $(s_i - s_i^{\text{ref}})$ is unchanged, hence

$$\tilde{p}_\theta(i|S_x) = \frac{\exp((s_i - s_i^{\text{ref}})/\tau)}{\sum_{j \in S_x} \exp((s_j - s_j^{\text{ref}})/\tau)}$$

is invariant.

Plackett–Luce teacher invariance. Let $q(i|S_x) \propto \exp(\hat{R}_i/\beta_r)$. For any constant $c \in \mathbb{R}$, if $\hat{R}_i \mapsto \hat{R}_i + c$ for all $i \in S_x$, then both numerator and denominator are multiplied by the same factor e^{c/β_r} , so $q(i|S_x)$ is unchanged.

Loss invariance. Since both $q(\cdot|S_x)$ and $\tilde{p}_\theta(\cdot|S_x)$ are invariant to groupwise additive shifts, the anchored listwise cross-entropy $-\sum_i q(i|S_x) \log \tilde{p}_\theta(i|S_x)$ is invariant as well. \square

C Implementation and Training Details

C.1 Noise Generation Procedures

We provide complete mathematical specifications for the four noise families used in our experiments.

Heavy Noise (Gaussian with outliers). For each item i in group S_x , the observed noisy reward is:

$$\tilde{R}_i = R_i^* + \epsilon_i,$$

where $R_i^* = f_\star(c, v_i)$ is the ground-truth reward from the oracle MLP f_\star , and

$$\epsilon_i \sim \begin{cases} \mathcal{N}(0, \sigma^2) & \text{with probability } 1 - p_{\text{out}}, \\ \mathcal{N}(0, \sigma_{\text{out}}^2) & \text{with probability } p_{\text{out}}, \end{cases}$$

with $\sigma_{\text{out}}^2 = 100\sigma^2$. The severity levels correspond to:

- Light: $\text{SNR} = \frac{\text{Var}[R^*]}{\sigma^2} = 1.0$, $p_{\text{out}} = 0.05$
- Medium: $\text{SNR} = 0.5$, $p_{\text{out}} = 0.10$
- Heavy: $\text{SNR} = 0.2$, $p_{\text{out}} = 0.20$

Distribution Shift. Training and test distributions differ in the context space. Let (c, v_i) denote training instances. Test instances are generated as:

$$(c_{\text{test}}, v_i) = (\alpha \cdot c + \delta \cdot \mathbf{1}, v_i),$$

where $\alpha > 1$ scales the context magnitude and δ adds a constant shift. Severity levels:

- Light: $\alpha = 1.2$, $\delta = 0.3$
- Medium: $\alpha = 1.5$, $\delta = 0.5$
- Heavy: $\alpha = 2.0$, $\delta = 1.0$

The ground-truth model f_\star trained on the original distribution must generalize to these shifted contexts.

Adversarial Label Flips. For pairwise comparisons (i, j) , we flip the preference label with probability p :

$$y_{ij}^{\text{flip}} = \begin{cases} 1 - y_{ij} & \text{with probability } p, \\ y_{ij} & \text{with probability } 1 - p, \end{cases}$$

where $y_{ij} = \mathbb{I}(R_i^* > R_j^*)$ is the clean label. For soft labels, we apply:

$$q_{ij}^{\text{flip}} = \begin{cases} 1 - q_{ij} & \text{with probability } p, \\ q_{ij} & \text{with probability } 1 - p. \end{cases}$$

Severity levels: Light (5%), Medium (10%), Heavy (20%).

Heavy-Tailed Noise (Cauchy). The observed reward is:

$$\tilde{R}_i = R_i^* + \epsilon_i, \quad \epsilon_i \sim \text{Cauchy}(0, \gamma),$$

where $\text{Cauchy}(0, \gamma)$ has PDF $f(\epsilon) = \frac{1}{\pi\gamma(1+(\epsilon/\gamma)^2)}$. This distribution has undefined mean and variance, making it particularly challenging. Severity levels:

- Light: $\gamma = 0.3$
- Medium: $\gamma = 0.5$
- Heavy: $\gamma = 1.0$

C.2 Hyperparameters and Training Configuration

C.3 Metrics Definition

WinMass. WinMass is defined as the expected probability mass assigned to the ground-truth best item:

$$\text{WinMass} = \mathbb{E}_{x \sim \mathcal{D}_{\text{test}}, S_x} [\tilde{p}_\theta(i^* | S_x)],$$

where $i^* = \arg \max_{i \in S_x} R_i^*$ is the item with the highest ground-truth reward. For random selection with $P = 4$ candidates, the baseline WinMass is $1/P = 0.25$.

D Additional Experiments and Ablations

D.1 Statistical Significance Tests

Method. For each scenario and method, we report mean WinMass over 10 random seeds. We compute 95% confidence intervals using the bootstrap method with 10,000 resamples. To test whether ADPO significantly outperforms Standard DPO, we use the paired Wilcoxon signed-rank test on the 10-seed results. The null hypothesis is that the median difference is zero. We report p -values and reject H_0 at $\alpha = 0.05$.

D.2 Effect of Reference Initialization

Ablation results. We evaluate ADPO performance with varying reference pre-training steps $N \in \{0, 10, 30, 100\}$ on Heavy Noise-Medium scenario. Results show ADPO maintains 8–15% advantage even with random reference ($N = 0$), confirming that the anchoring structure itself matters beyond initialization quality. Full pre-training ($N = 100$) provides marginal additional gains (+2–3%), suggesting that geometric centering is the key factor rather than reference quality alone.

Table 9: Complete hyperparameter configuration for all experiments.

Parameter	Value
<i>Optimization</i>	
Optimizer	AdamW
Learning rate	5×10^{-4}
β_1	0.9
β_2	0.999
Weight decay	10^{-4}
Learning rate schedule	Constant (no decay)
Batch size	32
Training epochs	80
<i>Model Architecture</i>	
Context dimension D_c	8
Item embedding D_v	8
Small model hidden	64
Medium model hidden	128
Large model hidden	256
Small model layers	2
Medium model layers	3
Large model layers	4
Activation	ReLU
<i>ADPO-specific</i>	
Temperature β	1.0
Temperature β_r	1.0
Listwise temperature τ	1.0 (pairwise), grid-search (listwise)
Reference pre-train steps	30 (on clean data)
<i>Experimental (Contextual Bandit)</i>	
Candidate set size P	4
Number of seeds	10
Training dataset size	10,000 instances
Test dataset size	1,000 instances
<i>Distillation Experiment (MuJoCo)</i>	
Teacher network	SAC with 512-512-256 hidden dims
Student network	256-256 hidden dims
Action candidates K	8
Distillation dataset	10,000 states
Training epochs	200
Batch size	128
Number of seeds	5
Teacher sampling ratio	75% (teacher) + 25% (random)

D.3 Temperature Sensitivity (Full Grid)

Figure 5 in the main text shows three representative methods. The full temperature grid for all methods is provided in the supplementary materials. Key findings:

- Pairwise-ADPO maintains $\text{WinMass} \in [0.61, 0.62]$ across all $(\beta_r, \tau) \in \{0.5, 1, 2, 4\}^2$;
- Listwise-Raw shows similar robustness ($\text{WinMass} \in [0.58, 0.63]$);
- Listwise-KDE benefits from lower τ (0.5–1.0) but degrades at $\tau > 2.0$.

D.4 KDE-CDF-Logit Transform Details

Given rewards $\{\tilde{R}_i\}_{i=1}^P$ in a group, ADPO-KDE constructs targets via:

1. **KDE fit (Scott’s rule).** Fit a Gaussian KDE $\hat{f}(r) = \frac{1}{Ph} \sum_{i=1}^P K(\frac{r-\tilde{R}_i}{h})$ with K standard normal and bandwidth $h = P^{-1/5} \hat{\sigma}$ (Scott’s rule), where $\hat{\sigma}$ is the sample standard deviation.
2. **CDF evaluation.** Compute $\hat{F}(\tilde{R}_i) = \int_{-\infty}^{\tilde{R}_i} \hat{f}(r) dr$.
3. **Logit map with clipping.** Let $\hat{F}_\epsilon(\tilde{R}_i) = \text{clip}(\hat{F}(\tilde{R}_i), 10^{-6}, 1 - 10^{-6})$ and $\ell_i = \log \frac{\hat{F}_\epsilon(\tilde{R}_i)}{1 - \hat{F}_\epsilon(\tilde{R}_i)}$.
4. **Temperature-softmax target.** Center logits via $\bar{\ell} = \frac{1}{P} \sum_j \ell_j$ and set

$$q(i|S_x) = \frac{\exp((\ell_i - \bar{\ell})/\beta_r)}{\sum_j \exp((\ell_j - \bar{\ell})/\beta_r)}.$$

This rank-like transform bounds outlier influence through the CDF and preserves separability via the logit.

E Reproducibility Checklist

To facilitate reproduction of our results, we provide the following information:

Random seeds. All experiments use seeds $\{0, 1, \dots, 9\}$ for 10-seed runs. Each seed controls:

- PyTorch random number generator: `torch.manual_seed(seed)`
- NumPy random number generator: `np.random.seed(seed)`
- Python built-in random: `random.seed(seed)`

Dataset generation. Synthetic contextual bandits are generated as follows:

- Context $c \sim \mathcal{U}[0, 1]^{D_c}$ with $D_c = 8$;
- Item embeddings $v_i \sim \mathcal{U}[0, 1]^{D_v}$ with $D_v = 8$;
- Ground-truth rewards $R_i^* = f_\star(\text{concat}(c, v_i))$ where f_\star is a 2-layer MLP with hidden dimension 64;
- Noisy observations \tilde{R}_i generated according to Section C.

Fixed random generation ensures identical train/test splits across all methods.

Code and configuration. Code and configuration files are provided in the supplementary materials. The repository includes:

- Implementations of all ADPO variants (pairwise/listwise, soft/hard);
- Standard DPO baseline implementation;
- Noise generation scripts for all four families;
- Experimental configuration YAMLS;
- Plotting scripts for all figures;
- Pre-computed results for verification.

Evaluation procedure. For each trained model:

1. Generate 1,000 test instances using the same distribution as training (or shifted distribution for Distribution Shift scenarios);
2. For each instance, sample $P = 4$ candidates;
3. Compute WinMass as $\mathbb{E}[\tilde{p}_\theta(i^*|S_x)]$ over all test instances;
4. Report mean and standard deviation over 10 random seeds.